universität wien

MASTERARBEIT / MASTER'S THESIS

Titel der Masterarbeit / Title of the Master's Thesis

„*Isolation and structural elucidation of natural components combined with metabolomic profiling in the Rudgea genus*“

verfasst von / submitted by

Lucia Schmidtbauer, BSc

angestrebter akademischer Grad / in partial fulfilment of the requirements for the degree of

Master of Science (MSc)

Wien, 2021 / Vienna 2021

Studienkennzahl lt. Studienblatt / degree programme code as it appears on the student record sheet:	A 066 862
Studienrichtung lt. Studienblatt / degree programme as it appears on the student record sheet:	Chemie
Betreut von / Supervisor:	Univ.-Prof. Dipl.-Chem. Dr. Lothar Brecker Privatdoz.

STATUTORY DECLARACTION

I hereby declare that the thesis submitted is my own unaided work, that I have not used other than the sources indicated, and that all direct and indirect sources are acknowledged as references.

This printed thesis is identical with the electronic version submitted.

Place, Date

Signature

ACKNOWLEDGEMENT

To begin with, I want to thank my supervisor Univ.-Prof. Dipl.-Chem. Dr. Lothar Brecker, Privatdoz. for offering me to work on this exciting topic. I am especially grateful for his advice and expertise whenever I was stuck with a problem. Also, I enjoyed the possibility to take part at several events like the “Österreichischen Chemietage”, it was a pleasure to work in such a friendly environment.

A special thanks goes to my coworkers at the Department of Botany and Biodiversity Research Vienna. For providing me the plant material, as well as the interesting and amusing discussions we shared during lunch and coffee breaks. I really appreciated the great supervision of Dr. Johann Schinnerl in my practical work in the laboratory as well as his fascinating talks about the world of Botany.

I also want to thank my working group colleagues at the Organic Chemistry Department for their countless advice and help with my NMR measurements, as well as for the fun we had at several trips and joint activities.

Furthermore, I want to thank the the NMR Center and the Mass Spectrometry Center of the University of Vienna for measuring all my samples. For the metabolomic profiling of my plant extracts I want to thank Univ.-Prof. Dr. Christopher Gerner and Julia Brunmair of the Department of Analytical Chemistry.

Finally, I want to thank my family, for financially supporting and encouraging me at all times. A very special thanks goes to my sister Katharina as well as my friends Jakob, Katharina, Fanny and Lea. Thank you for making my student years so eventful and exciting, for always motivating and believing in me and for the countless hours of advice and the distraction when I desperately needed it.

ABSTRACT

Phytochemical investigations of methanolic extracts, obtained from of *Rudgea* species led to the identification of four known secoiridoid glycosides and two unknown alstrostine derivatives: Isoalstrostine B and C. Their general structure is characterised by a pyrrolidinoindoline core and a tryptamine to iridoid ratio of 1:2. However, the novel alstrostines differ from the previously known representatives of this class by an additional caffeic acid attached to the 6''-position of the respective iridoid moiety. The two newly discovered isoalstrostines differ slightly from each other in one of the iridoid moieties. Variant B is equipped with an ester and an acid functional group represented in the respective secologanin, whereas the C variation is characterised by two acids as functional group.

Metabolomic profiling lead to the identification of several strictosidine derivatives in various Rudgea species. The minor presence of these metabolites suggests, that alstrostine producing plant species indeed have an active synthase catalysing the biosynthesis of strictosidine derivatives. However, their rare accumulation indicates they have little purpose in the plant.

Altogether, the plant species *R. skutchii* and *R. raveniana* accumulate great amounts of isoalstrostines, secologanin and its derivatives. This implies the accumulation of secologanin, which cannot be biosynthesised to strictosidine in the extent usual for Palicoureeae plant species. The discovered isoalstrostines are an important addition to the alstrostine structural group and underline their significance in the plant metabolism.

ZUSAMMENFASSUNG

Bei der phytochemischen Untersuchung von alkoholischen Extrakten von Pflanzenmaterial der *Rudgea* Arten konnten vier bekannte Secoiridoidglykoside und zwei bis jetzt unbekannte Alstrostinderivate isoliert werden. Die bekannten Vertreter der Alstrostine zeichnet sich durch eine Pyrrolidinoindolin-Grundstruktur und ein Tryptamin und Iridoid Verhältnis von 1:2 aus. Die beiden neuen Isoalstrostine, B und C, weisen eine zusätzliche Kaffeesäure auf, die an die an der 6''-Position der zweiten Glukoseeinheit gebunden ist. Die beiden neu isolierten Isoalstrostine unterscheiden sich dabei untereinander in der ersten Iridoideinheit: Isoalstrostine B charakterisiert sich durch einen Ester an Position 22, Isalstrostine C hingegen weist hier eine Säuregruppe auf. Beide Vertreter sind in Position 22‘‘ mit einer Säuregruppe ausgestattet.

Mit Hilfe von „Metabolomic profiling“ konnten verschiedene Strictosidinderivate in geringen Mengen in verschiedenen *Rudgea* Arten identifiziert werden. Das Vorkommen der Derivate in dieser Pflanzengattung weist auf das Vorliegen einer aktiven Synthase hin, die in geringem Ausmaß Strictosidin zu synthetisieren scheint. Die spärliche Anreicherung in den Alstrostin produzierenden Pflanzenarten deutet allerding auf geringe Bedeutung für die Pflanze selbst hin.

Im Rahmen dieser Arbeit konnte somit gezeigt werden, dass die beiden Pflanzenarten *R. skutchii* and *R. raveniana* sowohl große Mengen an Isoalstrostinen als auch Secologanin und dessen Derivate akkumulieren. Dies impliziert die Anreicherung von Secologanin in der Pflanze, welches nicht, im für Palicoureeae Pflanzenarten üblichen Ausmaß, zu Strictosidin weiter synthetisiert werden kann. Die beiden neu isolierten Isoalstrostine sind eine wichtige Ergänzung zur relativ neuen Strukturgruppe der Alstrostine; sie unterstreichen deren Bedeutung im Metabolismus dieser Pflanzenarten.

CONTENT

1. INTRODUCTION

1.1 Rudgea skutchii, Rudgea laevis and Rudgea raveniana

The species *Rudgea skutchii* Standl., *R. laevis* C.M. Taylor and *R. raveniana* W.C. Burger belong to the neutropically distributed genus *Rudgea* representing up to 120 species.[1,2] It is currently assigned to the tribe Palicoureeae which is a huge group within the coffee family (Rubiaceae).[3] Comprising over 13,000 species and more than 600 genera, the coffee family counts to the top five in terms of species-richness. The plant family exhibits diverse botanical characteristics reaching from small, weedy herbs to large rainforest trees. Members of the tribe Palicoureeae offer diverse biosynthetic routes producing and accumulating various chemical substances.[4]

The most prominent representative of the Rubiaceae family is the species *Coffea arabica* L., known as “coffee”. Caffeine is the chemical component responsible for its popular energizing effect. It acts as a stimulant of the central nervous system and is also used in the pharmaceutical industry for the production of migraine drugs.[5] Several species of Rubiaceae show psychogenic properties like *Psychotria viridis* Ruiz & Pav., which can be used as an adjuvant plant in the preparation of the traditional ‘ayahuasca’ drink. Traditionally, this drink is prepared by boiling or soaking psychotropic plants for instance the vine *Banisteriopsis caapi* (Malpighiaceae) with leaves of *Psychotria viridis*. While the *N,N*-dimethyltryptamine (DMT) present in the adjuvant plant is the psychoactive part of the brew, ß-carboline alkaloid derivatives inhibit monoamine oxidase (MAO). The inhibition prevents the degradation of DMT.[6]

With 24%, Psychotrieae and Palicoureeae represent most of the species in the Rubiaceae family. These genera play an important role in several terrestrial tropical ecosystems. Their fruits are important nutritional sources for various tropical birds and mammals, attracting them with their fruit texture and colour. The sister tribes differentiate morphologically by their stipules and biochemically by the presence of cyclotides. These peptides possess a broad range of biological activities and so far have only been found in Palicoureeae.[7]

In the Rubiaceae family the two large genera *Palicourea* and *Psychotria* evince extensive phytochemical investigations. *Rudgea* however, lacks equivalent data. Species belonging to the genus *Rudgea* are distributed from Mexico to Argentina. The

most diverse regions of their occurrence are in the states of the Southeastern region, Bahia and Amazonas. Typical characteristics of this genus are irregular domatia in the axils of the secondary veins, white flowers of different corolla shapes, pyrenes with pre-germinations slits and terminal inflorescences. The genus is usually determined by the appearance of glandular appendages.[1,8] Studies on the phytochemistry of *Rudgea* species are limited, in *R. jasminoides* and *R. viburnoides* (Cham.) Benth.. Naphtohydroquinone and triterpene derivatives have been identified. Latest studies of *Rudgea cornifolia* (Kunth) Standl. show the presence of alstrostines, a novel type of monoterpenoid alkaloids.[9]

1.2 Phytochemical aspects

Phytochemistry as a subfield of chemistry and botany focuses on the exact chemical constitution of plants and their biosynthetic metabolism. The metabolism of plants is divided in a primary and secondary part. While the primary metabolism is necessary for the development and growth of the plant, the metabolites of the secondary are mainly for its interaction with the environment. Some act as repellents against herbivores or as antioxidants against oxidative stress. The group of secondary metabolites can be generally sub-divided in alkaloids, phenols and terpenoids.[10]

1.2.1 Monoterpenoid indole alkaloids

Together with Apocynaceae species, species belonging to the tribe Palicoureeae comprise the biggest variety of monoterpenoid indole alkaloids (MIAs). MIAs can also be assorted as tryptamine-iridoid or terpenoid indole alkaloids. They show several useful properties and therefore their representatives such as camptothecin, vinblastine, vincristine and ajmaline. They can be used as anti-tumour-, anti-cancer treatment or as cardiac arrythmia medication.[11] Terpenoid indole alkaloids were classified to be derived from strictosidine. Strictosidine itself is formed from tryptamine and secologanin catalyzed by strictosidine synthase (STS) in a Pictet-Spengler condensation.[12]

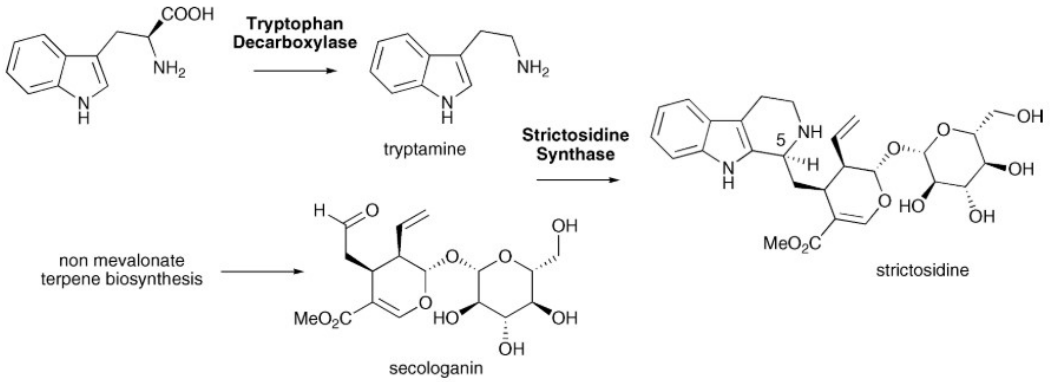

Figure 1. Biosynthetic route of strictosidine modified from O'Connor et.al., (2006).[11]

The first step is the decarboxylation of the L-amino acid tryptophan to tryptamine by the enzyme tryptophan-decarboxylase. Tryptamine subsequently reacts with secologanin to form strictosidine by condensation as shown in Figure 1.[13] In the order Gentianales, which comprises the coffee- and the dogbane family (Apocynaceae) together with other less speciose plant families, strictosidine-derived alkaloids have been investigated and described in wide variety of plant species.[12]

1.2.2 Secoiridoid glycoside

The starting component, secologanin plays an important role for the biosynthesis of MIAs as well as for other more complex alkaloids. The isoprenoid glycoside is a starting compound for the formation of the characteristic C9–C10 unit in the majority of indole alkaloids, some quinolines and isoquinoline alkaloids. It consists of a secoiridoid unit attached to ß-D-glucose by an *O*-glycosidic bond. Compounds derived from secologanin often exhibit a high degree of biological activity and are used as pharmaceuticals.[14]

As shown in Figure 2, the biosynthesis of secologanin starts with the formation of isopentenyl pyrophosphate (IPP) in the methylerythritol phosphate pathway (MEP). IPP is transformed into its isomeric form: Dimethylallylpyrophosphate (DMAPP). Two DMAPP units then form geraniol, an important intermediate in the biosynthesis. It is hydroxylated and further processed to yield loganin; secologanin synthase then catalyses the reaction to generate secologanin.[15]

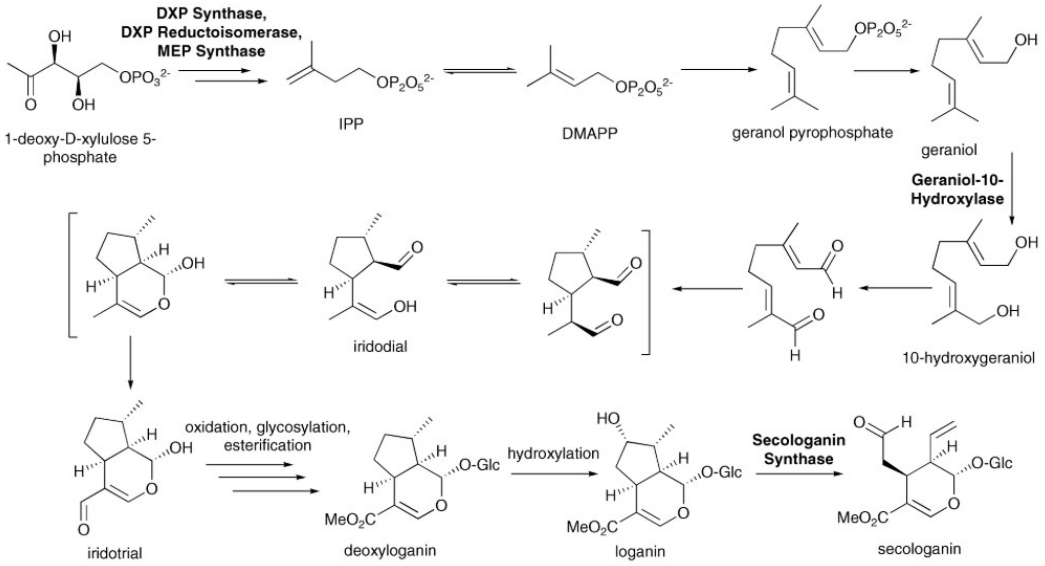

Figure 2. Biosynthesis of secologanin. The scheme shows the steps from the starting material 1-deoxy-D-xylulose 5-phosphate to secologanin, a precursor for secoiridoid. O'Connor et.al., (2006).[11]

Some of the derivatives of secologanin are secoiridoid glycosides, which are generally associated with a bitter taste and several bioactive properties. In Figure 3 simple representatives are shown. Secoiridoids like sweroside and swertiamarin have been used for anti-inflammatory, antiviral and antioxidative treatment.[16] The plant itself benefits from them i.e. in defence mechanisms against pathogens. The compounds are generally stored in a glycosylated nontoxic form in the vacuole, spatially segregated from the ß-glucosidase. Cell disruption caused by pathogen attack cancels out the discrete localization and therefore enables the ß-glucosidase to de-glycosylate the metabolite. The resulting aglycone is rather unstable and converts immediately to a highly reactive dialdehyde.[17] The aldehyde shows strong cross-linking / protein denaturing properties and cytotoxic effects.[18]

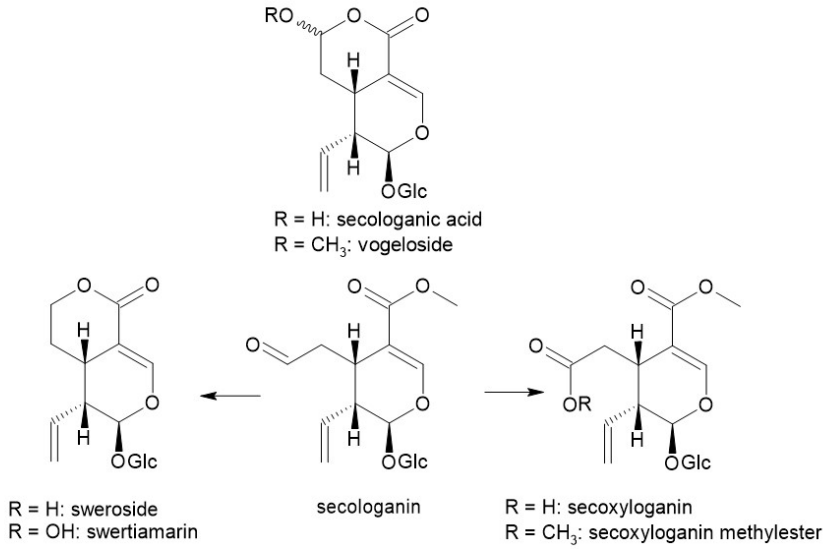

Figure 3. Several secoiridoid glycosides with its precursor secologanin.[19]

1.2.3 Alstrostines

Some recently discovered MIAs, the alstrostines, don't seem to be derived from the precursor strictosidine. The structural group comprising one tryptamine and two iridoid units are a rather novel structural group.[13] Representatives have only been found in four different plant species. Alstrostine A was found in *Alstonia rostrata* C.E.C. Fisch. (Cai et al., 2011) (Apocynaceae), *Chassalia curviflora* var. *ophioxyloides* (Wall.) Deb & B. Krishna (Rubiaceae) (Schinnerl et al., 2012), dehydro-rudgeifoline and isoalstrostine A in *Palicourea luxurians* (Rusby) Borhidi (Kornpointner et al., 2020) and rudgeifoline was isolated from *Rudgea cornifolia* (Schinnerl et al., 2012).[3,9,13,20] They distinguish from the strictosidine-type alkaloids in their different tryptamine to iridoid ratio of 1:2, as well as in their pyrrolidinoindoline core. These differences indicate an unknown biosynthetic pathway opening new possible routes for specialized metabolites within the studied taxa. The different biosynthesis route could be a result of the STS-synthase being inactive or rather another enzyme catalysing the synthesis. However, previous studies assume the presence of STS but question its substrate promiscuity.[13]

The biosynthesis of this novel subclass is not yet well understood. In Figure 4 the proposed biosynthesis route is shown. It is assumed, that first L-tryptophan undergoes cyclisation and oxidation to form the alline-like intermediate with two

secondary imine units. Subsequently, both imines each react with a respective secologanin unit to form enamines. It is critical which of the enamine functions gets protonated in the next step (d1/d2). The formation of the second six-membered ring determines whether an isoalstrostine (d1) or an alstrostine (d2) is synthesized.[13,20]

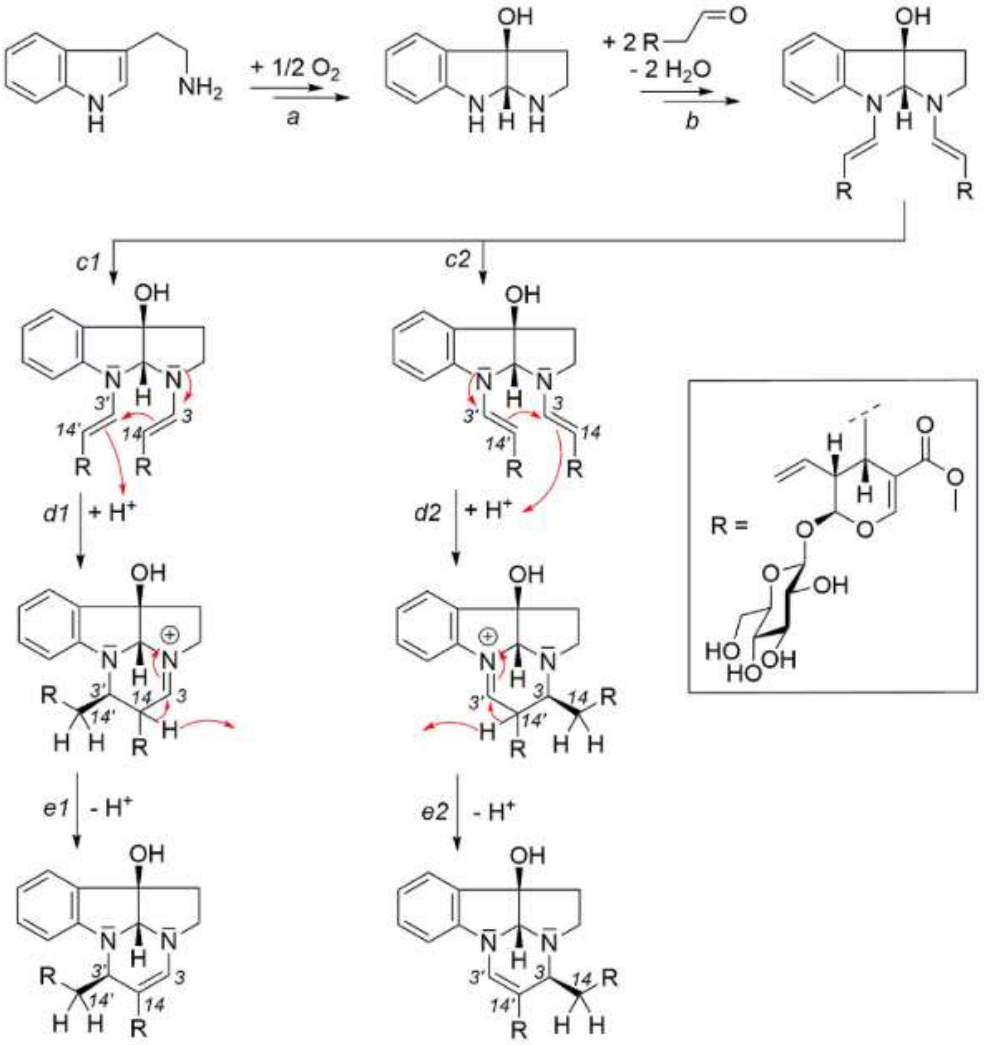

Figure 4. Biosynthesis of isoalstrostine and alstrostine. Kornpointner et.al., (2020)[13]

1.3 Aim of this work

The present work aims to further understand the chemical diversification within the *Psychotria* alliance and focuses on the hardly investigated *Rudgea skutchii*, *R. laevis and R. raveniana.* Both leaves and stem material of the neotropically distributed species were used for the analysis of their chemical composition.

The first and main part of this work was to isolate, purify and elucidate the structure of natural components from *Rudgea* species. Therefore, methanolic extracts of the leaves and stem material were investigated. The components in the crude extracts were separated by their lipophilia via liquid-liquid extractions with solvents of different polarities. The liquid extracts then are further purified by using several chromatographic methods as separating by size and again lipophilia. The progress was permanently monitored by thin-layer chromatography (TLC) and high-pressure-liquid chromatography (HPLC). Staining reagents and UV/Vis spectroscopic measurements provided first indication on the structural group and chemistry of the unknown compounds. If sufficient pure amount could be afforded, spectroscopic methods were employed to elucidate its structure. Mass spectrometry and one-dimensional nuclear magnetic resonance spectroscopy (NMR) were used to determine de molecular mass and its chemical formula. Two-dimensional NMR (COSY, TOCSY, NOESY, HSQC, HMBC) then was applied to determine the chemical structure and the stereochemistry of the molecules.

The second part targeted the investigation of the composition of the crude extracts. Screening for little amounts of known substances in the methanolic extracts of *Rudgea* samples. Purifying the desired compounds with chromatographic methods and then elucidating their structure by NMR would demand great amounts of sample. Even if the concentration of the natural component in the extract would be high enough, its successful separation from the other components is not guaranteed. Therefore, mass spectrometry, precisely metabolomic profiling, was used. The technique uses previously isolated and purified substances as standards and alcoholic extracts of leaf and stem material of *Rudgea* samples. It allows the determination of chemical components in a diverse matrix, even in very little amounts. Metabolomics was used to get a better impression of the chemical composition of plant species producing MIAs besides the well-studied strictosidine-pathway. Therefore, they could lead to a better understanding of the biosynthesis of those plant species.

2 MATERIAL AND METHODS

2.1 Methods for purifying and isolation of natural components

Several separation and preparation steps are necessary for the complete characterization of natural components in plant material. Chromatography and liquid-liquid extraction are the most established methods for isolation and purification of natural components in sufficient yield.[21]

2.1.1 Extraction methods

For a satisfactory isolation of secondary plant metabolites, the collected leaves or stem of the plants are air-dried, powdered and extracted with methanol (500 mL). To enhance the extraction, the plant material is soaked in methanol for three days. Extraction procedure is repeated three times, the extracts are combined, filtered and concentrated under reduced pressure. Evaporating the alcohol in a rotary evaporator is a very mild method to prevent the components from decomposing.[22]

Firstly, the residue was resuspended in H_2O and petrol ether (PE) was added to solve and remove the majority of the chlorophyll and lipophile components.[23] The remaining aqueous solution then gets further separated in a separating funnel by liquid-liquid extraction. The extraction with different solvents enables a crude pre-separation, which simplifies the chromatographic separation steps. The solvents polarity is increasing in each step, thus allowing a separation of the components by their polarity. By using a two-phase system of $CHCl_3$ and H_2O, the remaining nonpolar substances are transferred into the lipophile $CHCl_3$ phase. To abstract the polar constituents, first EtOAc and then *n*-BuOH is used. The residual water phase mainly holds sugars and other polar molecules.

The best approach to improve the extraction capacity is to use small amounts of solvent and repeat the extraction several times. The distribution of a component in a two-phase-system is described by the Nernst partition law shown in Equation 1.[24]

$$K_D = \frac{c_1}{c_2}$$

Equation 1

K_D Nernst partition coefficient

c_1 Concentration of substance A in phase 1 (mol L^{-1})

c_2 Concentration of substance B in phase 2 (mol L^{-1})

The relation given in Equation 1 determines the relative distribution of a compound between two immiscible - or miscible to minimum extent - solvents. When soluble in both liquids and at equilibrium, the concentration of the component in the two separate phases is constant.[24] Considering the fact that the concentration and solubility of unknown components of a crude extract are not known, the Nernst partition law can only be used as a first indicator. By using unsaturated extracting solvents, the concentration difference between crude extract and solvent is huge and therefore the yield of compounds in the extracting solvent is higher.

2.1.2 Chromatographic separation methods

After liquid-liquid extraction the natural components are relatively crude distributed by their polarity. By analysing the extracts with HPLC with coupled UV/Vis methods, one can get an overview of the composition of the liquid extracts. Fractions containing main amounts of target components can then be further separated and purified by chromatographic separation methods.

Generally, the constituents can either be separated by their polarity or their size. In this work, thin-layer chromatography (TLC), preparative thin layer chromatography (PTLC), column chromatography (CC), size-exclusion chromatography (SPE), medium-pressure liquid chromatography (MPLC) and high-performance liquid chromatography (HPLC) were used. The separation set consists of a stationary and mobile phase, the phases polarity is contrary and the stationary phase can either be normal or reversed phase. Normal phase chromatography (NPC) uses polar silica gel as stationary phase and nonpolar eluents, reversed phase chromatography (RPC) uses a chemically modified and therefore nonpolar stationary phase and polar mixtures as eluents. The substances interact with the stationary phase differently and the better the affinity, the better it binds to it and the later it gets eluted by the mobile phase.[25]

TLC is very commonly used. It enables a fast and easy separation and therefore is often used to overlook the progress of a separation by column chromatography. Usually the stationary phase consists of SiO_2 applied on a carrier material, generally aluminium or glass. Depending on the requested separation, the eluent is a mixture of several polar and nonpolar solvents. The separation can be observed in UV light or by using colouring reagents like anisaldehyde or Dragendorff's reagent.[26]

PTLC relies on the same principles as simple TLC - it is mostly used in final purification steps. The SiO_2 is applied on glass, thus enabling the recovery of the

components by scratching of the component bands. The natural components can be resorbed in solvent, i.e. methanol and separated from the stationary phase by filtering. The methanol is evaporated and the pure component is available for further use.[27]

Column chromatography is the most popular method for separating natural components of plant extracts. Finely powdered silica gel is used as stationary phase (normal or reversed phase) and several solvent or mixtures of them operate as mobile phase. Normal phase is combined with methanol or mixtures of MeOH with EtOAc or $CHCl_3$, reversed phase is eluted with a mixture of H_2O and MeOH.[28]

MPLC is another way to separate natural components. The use of a pump as a solvent delivery system allows a more controllable separation. The operating pressure usually is about 5 to 40 bar and particle size ranges from 25–40 µm. The stationary phase can be normal or reversed phase.[27]

As the name suggests, the separation of size exclusion chromatography (SEC) relies on the different size of the molecules. The stationary phase consists of macroporous polystyrene / divinylbenzene copolymers, the size of the pores is strictly restrained. Small molecules can enter the pores better than bigger ones and get temporarily “trapped”. Large molecules pass through the stationary phase rather unhindered. The retention time of the components relates to their molecular size. [27] In this work a dextran-epichlorohydrin copolymer called Sephadex (Separation Pharmacia Dextran) was used as stationary phase for size exclusion chromatography.[29]

Enhancement of separation can be achieved by varying the elution method. The use of isocratic or gradient elution can be crucial for separating similar polar components. In addition, CC, MPLC and SEC can be coupled with a UV detector. When the UV maxima of the desired compound has been determined, the detector can detect the arrival of the fraction carrying the compound of interest. This enables rather accurate fractioning.[30]

2.2 Methods for characterization of natural compounds

Successfully isolated and purified natural compounds show several characteristics by which they can be identified and compared. For novel natural components, the elucidation of their structure as well as three-dimensional positioning and the determination of their molecular weight are essential. Additional attributes can be an important and helpful tool for chemists and botanists to distinguish different natural components.

2.2.1 UV/Vis spectroscopy

UV/Vis measurement offers information about chromophores present in the sample, some natural components show characteristic absorption peaks. For instance, flavonoids and alkaloids can be determined by their UV maxima.[27]

Furthermore, an isolated, pure compound can be characterised by its molar decadic extinction coefficient ε. As visible in Equation 2, ε can be determined by detecting the extinction rising by the compound in solution: The concentration of the compound solution, as well as d, I_0, I_I are set, E is determined and therefore the compound specific parameter, ε, can be calculated. Measurements are performed in a photometer, the sample is transferred in a quartz cuvette and the solvent has to be declared as it can influence the absorption.[26,25]

$$E = \log\left(\frac{I_0}{I_I}\right) = \varepsilon * c * d$$

Equation 2

E extinction

I_0 intensity of incoming light stream

I_I intensity of outgoing light stream

ε molar decadic extinction coefficient [L mol^{-1} cm^{-1}]

c concentration of substance [mol L^{-1}]

d optical path in the cell

2.2.2 HPLC-measurements

HPLC is a very effective tool for natural component isolation, it enables the tracking of the separation progress and depicts the purity of the analysed sample. The level of the analyte in the natural product matrix can be determined in every step of the process. Therefore, enriched fractions can be chosen for further isolation steps. The measuring method should be designed at the beginning of the extraction work and should be used for all measurements, thus enabling comparison of the retention time and UV absorption spectra of several natural components. Critical for the separation quality are parameters like injection volume, flow rate, temperature, choice of eluent, eluent gradient and column material as well as the compounds characteristics.

2.2.3 Polarimetry

Compounds with one or more stereocenter are optically active, meaning they can rotate the plane of polarization of plane-polarized light. Substances rotating the plane clockwise are regarded as dextrorotatory and those rotating it counterclockwise as levorotatory. The direction of the rotation is generelly referred to by the prefixes (+) for dextrorotatory or (-) for levorotatory substances. The specific optical rotation of a substance can be measured with a polarimeter. Most of them use a sodium arc as light source (sodium D-line, λ = 589 nm). The monochromatic light emerges as a plane-polarized light after passing through a polarized lens, when passing through the sample tube, its plane of polarisation can be rotated by optically active substances. The analyser determines the angle in rotation in °C, the specific rotation of the optically active compound can be calculated using the formula given in Equation 3.[31]

$$[\alpha]_D^{20} = \frac{observed\ rotation\ [°C]}{cell\ length\ [dm] * concentration\ [g\ 100\ mL^{-1}]}$$

Equation 3

2.2.4 Mass spectrometry

Mass spectrometry analysis determines the exact mass of molecules and can give a first indication of the structure and element constitution. High resolution time-of-flight (HR-TOF) was the method of choice to analyse secondary plant metabolites. The separation is based on the different time of flight of the molecules. They are accelerated on a drift tube and heavier molecules reach the detector later than more light weighted ones. For the Ionisation electron spray ionization (ESI) was used, it

enables soft ionisation and thereby only little fragmentation. Moreover, the molecules can be ionized in positive and negative mode.[32]

2.2.5 NMR spectroscopy

Nuclear Magnetic Resonance (NMR) enables the full structural elucidation of natural compounds, therefore they must have a high degree of purity and at least 1.5 mg are necessary. The dried isolation product is resuspended in deuterated solvents; thereby, the solvent will not affect the results and will not produce a signal.

NMR analysis is limited to nuclei with a spin quantum number other than zero, most popular representatives for these characteristics are ^{13}C and ^{1}H. The chemical shifts δ_C of ^{13}C measurements give a general idea on the structural skeleton of compounds. The proton NMR offers information on the chemical shift δ_H the multiplicity and the coupling constant *J*. Because of the natural abundance of 99.98% for ^{1}H and only 1.1% for ^{13}C, proton NMR has clear advantages. Furthermore, it convinces with higher sensitivity, and a shorter relaxation time. Due to its quick measuring time, ^{1}H NMR is often used as purity control of isolated compounds. The carbon NMRs are recorded in DEPT (distortionless enhancement by polarisation transfer) or in j-mode (j-modulated spin echo mode). While in DEPT the quaternary carbons are not shown at all, in j-mode one can differentiate the primary and tertiary carbons on the one side, and the quaternary ad secondary carbon atoms on the other side. For both 1D NMR methods, the chemical shift δ_H allows the identification of several functional groups and gives a crude idea about the atoms chemical surrounding. Additional two dimensional NMR experiments generate information on position and interaction of the atoms.[33,34]

COrrelated SpectroscopY (COSY) is a homonuclear experiment, i.e. shows the scalar coupling between two protons. Those scalar couplings result in crosspeaks, their intensity depends on the spatial distance between the atoms. The more atoms are in between, the less the intensity of the crosspeak. Another factor influencing the peak-intensity is the bond angle; the strength of the $^{3}J_{H\text{-}H}$ coupling reaches its maximum at a torsion angle of 0° or 180° and its minimum for vicinal coupling at 90°. The context of coupling strength and torsion angle is described by the Karplus equation. The different coupling strength is often very useful for distinguishing sugar units.[34,35]

TOtal Correlated SpectroscopY (TOCSY) is another homonuclear spectrum, assigning nuclei, which are not essentially connected by scalar coupling, to a secluded

spin system. It differs from COSY in its mode of acquisition, an additional spin lock in the mixing time results in propagation of the magnetisation alongside a continuous row of nuclei and therefore shows the coupling over several bonds. Natural components often consist of more than one structural element which are separated by quaternary carbons or heteroatoms. A TOCSY spectrum gives a crude idea about the different structural elements, which then have to be connected with other NMR methods.[35]

Nuclear Overhauser Effect SpectroscopY (NOESY) is the third homonuclear method, it detects spatial proximity of atoms without them being connected directly by bonds. The spectrum relies on the nuclear Overhauser effect which is dependent on the distance and the tumbling rate and therefore size of a molecule.[35]

Heteronuclear Single Quantum Correlation (HSQC) is, as its name suggests, a heteronuclear spectrum. It displays the coupling of carbons with protons. It is a convenient start for structural elucidation with NMR because it correlates the protons to its corresponding attached carbon. Also, it determines quaternary carbons, as they show no $^{1}J_{C\text{-}H}$ coupling.[35]

Hetero Multiple Bond Correlation (HMBC) is based on the same approach as HSQC, with the difference that it shows correlation of atoms over two to three bonds. Therefore, it enables the linking of single hydrocarbon fragments and especially the integration of quaternary carbons.[35]

2.3 Methods for determining trace amounts of metabolites in a diverse matrix

2.3.1 Metabolomic profiling

Metabolomics describes the analysis of small molecules (usually below 1500 Da) and characterization of the metabolome, i.e. the entire set of small metabolites in a biological sample or organism.[36,37] It is defined by its heterogenous composition and therefore diverse physical and chemical properties. Concentrations in the matrix, i.e. a biological sample or the environment, can range from trace to main amounts. Their polarity can range from hydrophile to hydrophobic, defining the subclasses of the metabolome: Metabolomics and lipidomics.[38]

The identification and quantification of the metabolome is referred as metabolic profiling.[39] The widely diverse properties make the analysis in fact quite challenging and the demand on highly accurate analytical instruments is great. NMR and MS are the analytical platforms of choice. NMR distinguishes with its high robustness,

rapidness and no need of an analytical standard, whereas the selectivity of MS makes it an effective tool for detection and quantification of small molecules in a complex biological sample. MS coupled with a prior separation unit like liquid chromatography (LC) enables an accurate and sensitive analysis of a wide range of diverse metabolites.[40]

The general approach for metabolomic profiling includes sample preparation, analysis and data processing. To detect defined metabolites in a biological matrix i.e. a plant extract, targeted data evaluation is the method of choice.[39] Thereby, the desired analytes are prepared as standards in appropriate concentrations and analysed by mass spectra. Raw MS data files can be processed with Tracefinder 4.1 (https://www.thermofisher.com/at/en/home/industrial/mass-spectrometry/liquid-chromatography-mass-spectrometry-lc-ms/lc-ms-software/lc-ms-data-acquisition-software/tracefinder-software.html) and Skyline 20.1 software (https://skyline.ms/project/home/software/Skyline/begin.view). The data are imported to the software and peak extraction is performed. Therefore, the product ion (i.e. the one with highest intensity or with specific character) must be determined for all metabolites as well as their exact retention time information. Then the extracts of interest are measured by MS as well and their spectra are imported into Tracefinder or Skyline, peaks in the extracts raw data are matched with the previously imported data. Afterwards a report is generated with all the information about the detected metabolites including the indexes metabolite name, molecular formula, sample name, measured retention time and area.[41]

3 EXPERIMENTAL

3.1 Extraction of the natural components

3.1.1 The crude extract

The plant material of *Rudgea skutchii* with the sampling number 1351, of *Rudgea raveniana* W. C. Burger (1413) and of *Rudgea laevis* (2024) was collected near La Gamba in Costa Rica by coworkers of the Department of Botany and Biodiversity Research Vienna. The leaves and stem material were separated and air dried under exclusion of light.

AB1351

The dried leaves were powdered and the dry weight of 72.9 g was determined. To the ground plant material 500 mL of MeOH were added and kept in a dark place at room temperature for three days. The obtained alcoholic extract was filtered and the residue was again covered with MeOH. This was repeated three times, the extracts were combined and concentrated under reduced pressure at a temperature of 38°C. The dried crude extract was weighed on a laboratory scale and amounted 4.4 g. A small part of the extract was resuspended in 10 mL MeOH and an aliquot of 350 µL was diluted with 250 µL MeOH. This diluted sample was used for the HPLC-measurement given in Figure 5. All following drying, and weighing procedures were conducted with the same conditions as described in this paragraph.

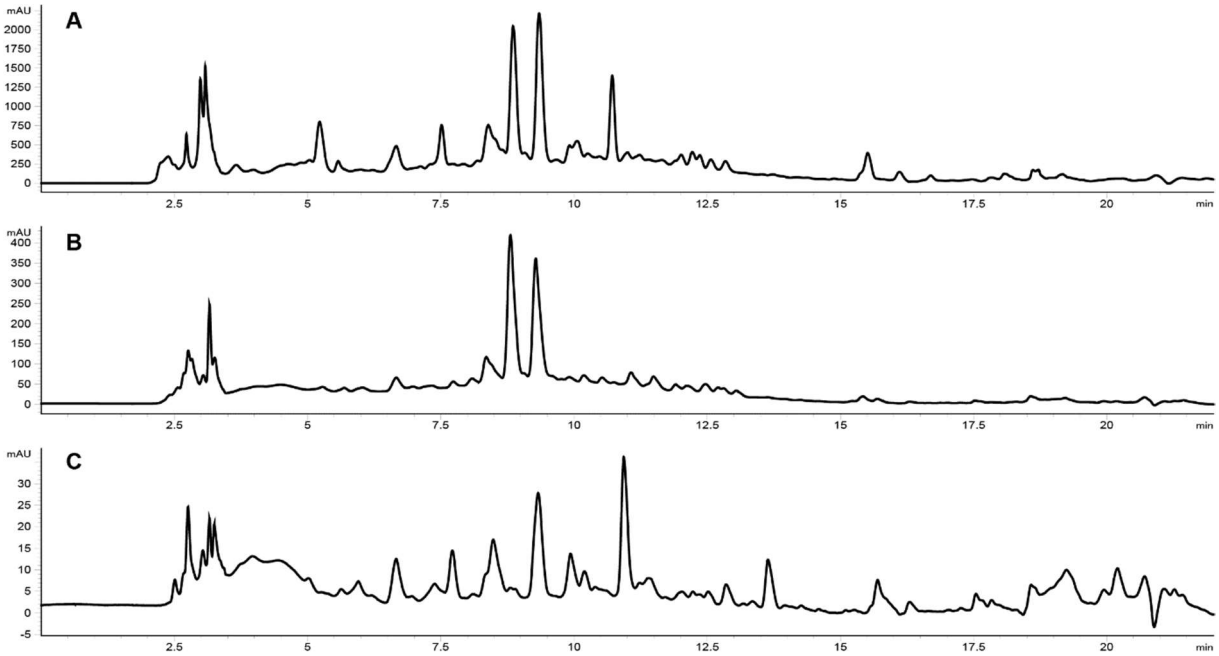

Figure 5. HPLC chromatograms of the methanolic crude extracts obtained from the leaves of the samples AB1351 (A), RUD1413 (B) and D2024 (C). The wavelength of detection was set at λ = 230 nm

C1351

The stem material was treated identically, as stated for the leaves above. The stems dry weight was 66 g and the afforded, dried extract 1.8 g. The resulting HPLC chromatogram is shown in Figure 6.

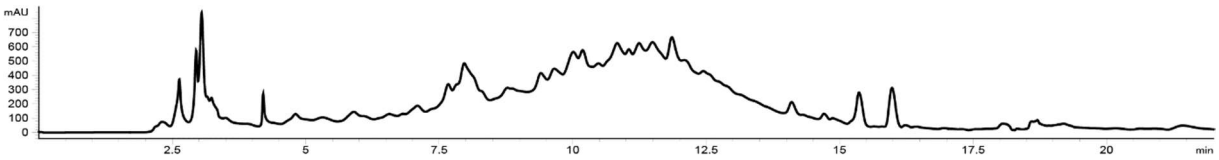

Figure 6. HPLC chromatogram of stem bark crude extract C1351, MeOH, λ = 230 nm

RUD1413lv and D2024

The plant material of Rud1413 weighed 74.6 g of which 5.5 g were gained as dry extract. From 30.5 g of the sample D2024 a dry mass of 3.8 g crude extract could be obtained. Both sampling materials were treated as described for AB1351. HPLC-chromatograms are shown in Figure 5.

3.1.2 First crude separation step of the extracts

As a first step, the dried crude extract was dissolved in 250 mL H_2O and covered with 250 mL PE and the dark green supernatant was removed. This was repeated four times. To the residual H_2O extract, 250 mL $CHCl_3$ were added. The non-miscible two-phase system was transferred in a separation funnel and shaken vigorously. The chloroform phase was separated and collected in a round bottom flask. This procedure was repeated four times with 250 mL chloroform each. The $CHCl_3$ extracts were combined, concentrated under reduced pressure and a HPLC chromatogram was recorded. The same steps were repeated with EtOAc (3x 250 mL) and *n*-BuOH (3x 250 mL). From these obtained organic phases and the remaining water phase, HPLC chromatograms were recorded.

All described steps were performed with extracts obtained from the samples AB1351, C1351 and D2023. In Table 1 all the resulting dry weights of the different extracts are listed.

Table 1. Dry weights of all liquid extracts. Liquid extraction was not performed on crude extract of RUD1413lv

	dry weights [g]					
sample	crude extract	PE	$CHCl_3$	EtOAc	*n*-BuOH	H_2O
AB1351	4.4	1	0.2	0.7	0.4	2.1
C1351	1.8	0.3	0.2	0.2	0.4	0.7
D2024	3.8	1	0.5	0.1	0.4	1.7
RUD1413lv	5.5	-	-	-	-	-

3.2 Isolation of plant constituents

Various chromatographic methods like column chromatography (CC) were performed in order to purify characteristic compounds from the extract. In Figure 7, an overview of the separation steps for extract AB1351 is depicted. The separation steps yielded four pure samples, which were investigated by mass spectrometry and NMR spectroscopy for structure elucidation.

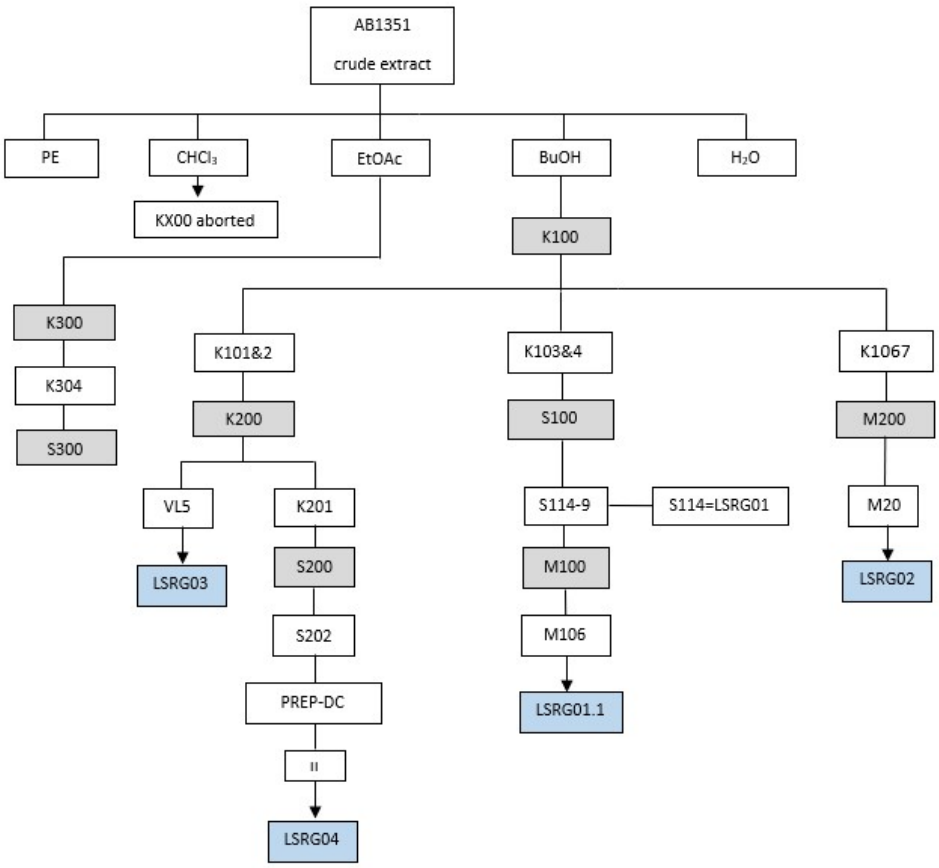

Figure 7. Chromatographic separation scheme of crude extract AB1351

The extract of the stem material of *R. skutchii* was also treated with several chromatographic methods to gain pure compounds, but only one fraction was pure enough for further investigations. The amounts of the remaining fractions were not sufficient for further purification steps.

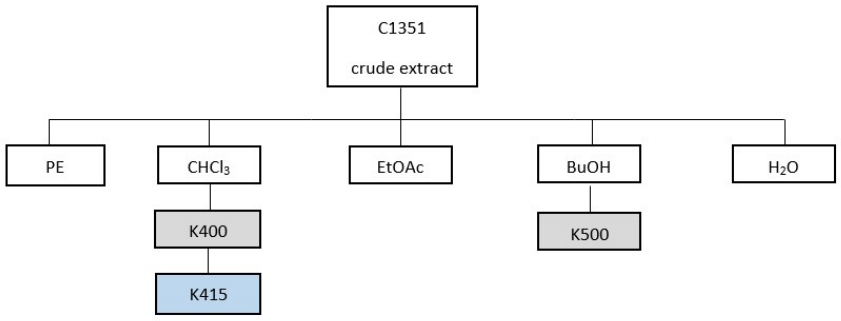

Figure 8. Chromatographic separation scheme of crude extract C1351

The third crude extract underwent the same liquid extractions as the others. However, as the HPLC chromatograms of the $CHCl_3$ phase and the EtOAc phase showed peaks with very similar UV-spectra, the chloroform extract was separated again. It was dried under reduced pressure and extracted with a mixture of PE/EtOAc 70:30 and H_2O three times. The H_2O extracts were combined, dried and merged with the EtOAc extract. With several chromatographic methods like column chromatography over silica gel and sephadex LH20 as stationary phase, it was possible to obtain one fraction which was pure enough for NMR and mass investigations.

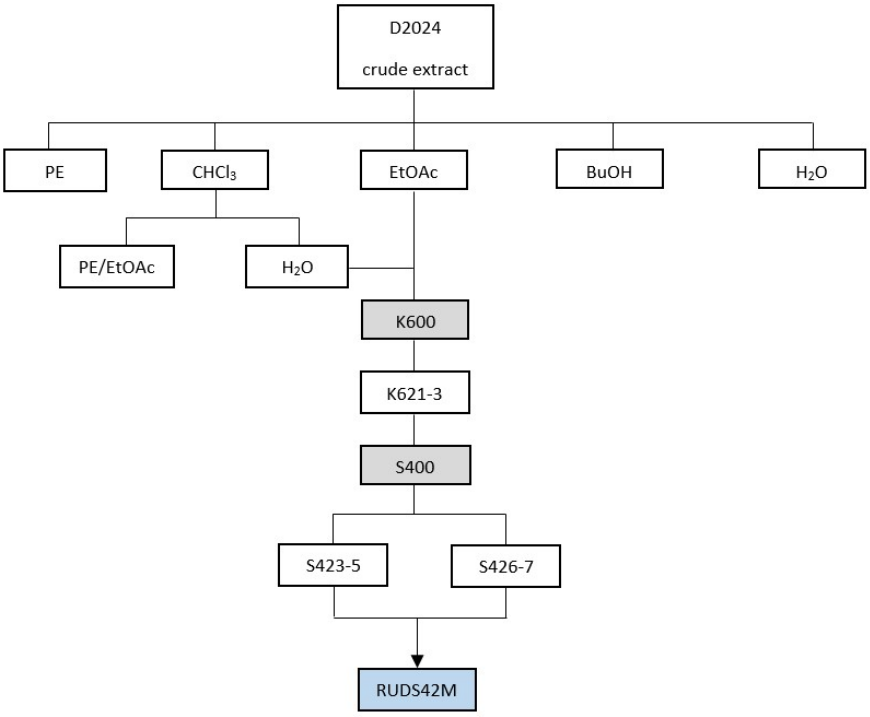

Figure 9. Chromatographic extraction scheme of crude extract D2024

3.2.1 Isolation of LSRG-01 (1)

For the isolation of LSRG-01 (**1**) the *n*-BuOH-phase was used due to its HPLC chromatogram (Figure 10). It was dissolved in MeOH and transferred onto a silica gel column (K100). Therefore, 20.8 g of silica gel (0.04–0.063 mm) were suspended in 100 mL of a mixture $CHCl_3$/MeOH (40:60) and filled in a column. The extract was eluted with 100 mL of this mixture and then with a gradient of 15% step for every 100 mL. The elution afforded 22 fractions of approximately 50 mL, which subsequently were analysed with HPLC and TLC (50:10:40 *n*-BuOH/glacial acetic acid/H_2O). The TLC plates were analysed under UV-light at 254 nm and for additional information treated

with an anisaldehyde solution and Dragendorff's reagent. The anisaldehyde solution had to be prepared first: Under ice cooling, 8 mL of H_2SO_4 were added to a mixture of 85 mL MeOH and 10 mL glacial acetic acid. Further on, 0.5 mL of anisaldehyde were added. The reagent had to be stored under 4° until further use. All the following developed TLC plates were treated the same as described above.

Based on the results from TLC plates and the HPLC-chromatograms the fractions K101&102 as well as K103&K104 and K106–107 showed promising UV-characteristics and were further separated. In the case of LSRG01 the fractions K103&104 were dried, dissolved in MeOH and transferred onto a pre-eluted sephadex column (MeOH, length: 75 cm, diameter: 1.2 cm). The separation was conducted with elution of MeOH and collecting fractions of approximately 30 mL. Fraction S114 was considered as pure enough and with a yield of 5.2 mg. From this fraction NMR analysis could be performed, but the ^{1}H NMR spectrum revealed its impurities. For refining of this sample, it was combined with fractions S115–119 (14.2 mg in total) and further purified by MPLC separation. The sample was dissolved in a few drops of methanol and some water was added. This solution was injected in the sample loop by using a syringe. It was eluted with a gradient starting with 98:2 H_2O/MeOH. In 10 mL steps, the amount of MeOH was increased by 5 % until it reached 25 %, then the column was eluted with pure MeOH. The flow rate was set at 7.5 mL min^{-1}. The column was connected to a UV-spectrometer, thus allowing the separation progress to be followed. The wavelength of detection was set at 206 nm and 326 nm. Finally, the resulting fraction M106 (LSRG01) (**1**) with the amount of 3.8 mg allowed detailed structure elucidation with NMR and MS methods. The chromatogram and the related UV absorption spectrum are depicted in Figure 11. The whole amount of 3.8 mg was dissolved in CD_3OD and transferred into an NMR sampling tube. A small droplet of the residual resolved sample was used for the MS-measurements which was conducted on a HR-ESI-TOF-MS. The NMR analysis included one-dimensional ^{1}H NMR and ^{13}C NMR, as well as the two-dimensional NMR methods COSY, TOCSY, HSQC, HMBC und NOESY.

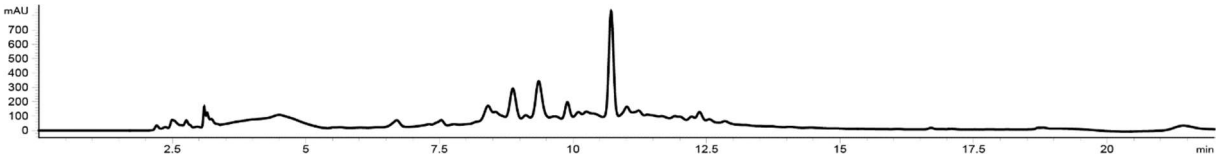

Figure 10. HPLC chromatogram of the *n*-BUOH phase of crude extract AB1351 in MeOH. The wavelength of detection was set at 230 nm.

Additionally, the decadic extinction coefficient, ε was determined by UV/Vis spectroscopy. The sample was diluted in MeOH to reach a concentration of 2.5 µL mL^{-1}, and the UV absorption measured at the respective UV maxima. From the obtained values for the extinction E, the molar decadic extinction coefficient ε could be calculated using Equation 2. With a polarimeter the optical rotation was determined. To obtain the specific rotation, the dried sample was dissolved in 2 mL MeOH (c = 1.9 mg mL^{-1}), the angle of rotation was determined and the specific rotation was calculated. The pure compound was dried under reduced pressure and stored at -20°C. All the following isolated compounds were stored the same way until further use.

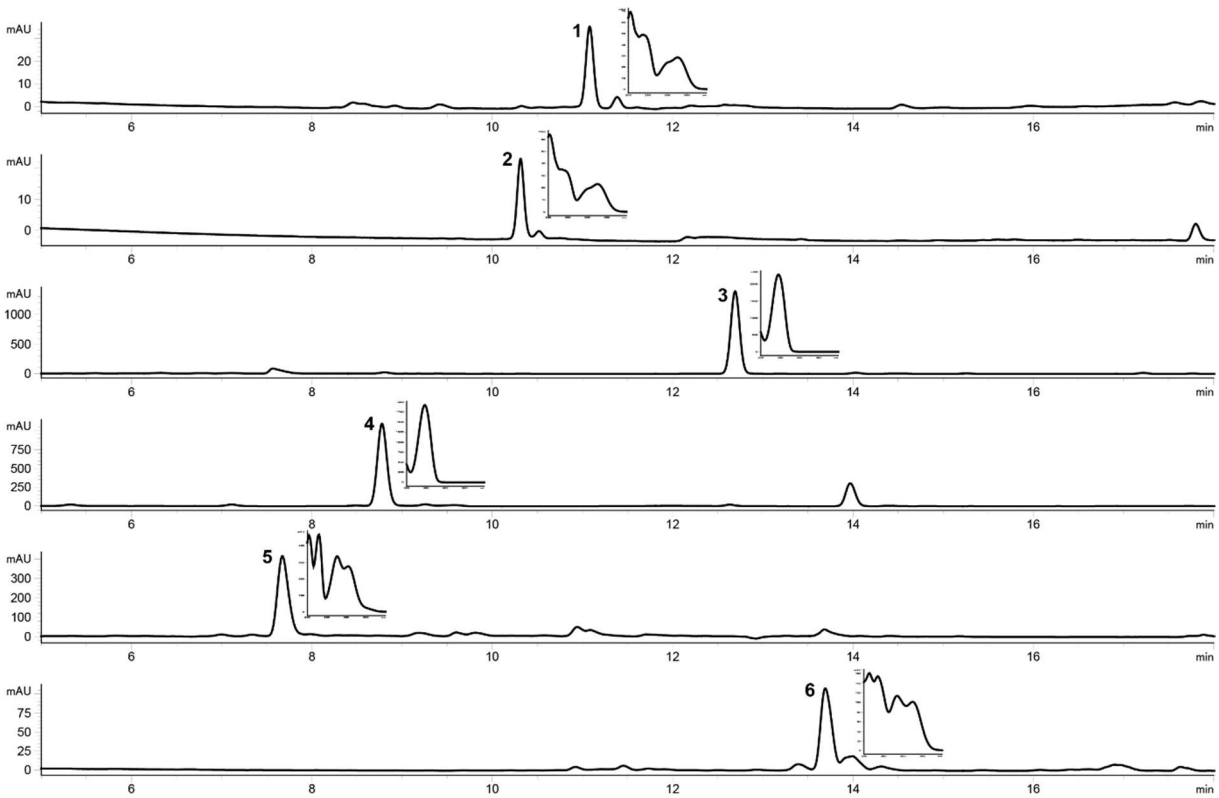

Figure 11. HPLC chromatograms of the isolated compounds LSRG-01 **(1)**, LSRG-02 **(2)**, LSRG-03 **(3)**, LSRG-04 **(4)**, K415 **(5)** and RUDS42M **(6)**, the UV spectra of the compounds is depicted next to the assigned peak. MeOH, λ = 230 nm

3.2.2 Isolation of LSRG-02 (2)

For the isolation of compound LSRG-02 (**2**), the fractions K106–8 (6.8 mg) of the first silica gel column K100 were further separated by MPLC. This reversed phase column was eluted with a gradient again, starting with 95:5 H_2O/MeOH. The gradient steps were 5% increase of MeOH per 50 mL. After 45:55 H_2O/MeOH, the column was eluted with 100% MeOH. The separation obtained 35 fractions out of which M206–212 and VL18 showed the desired compound in the HPLC chromatogram. These fractions were pooled (1.5 mg) and named as LSRG-02 and further analysed by NMR and mass spectrometry. As for compound LSRG-01 (**1**), the molar decadic extinction coefficient and the optical rotation were determined.

3.2.3 Isolation of LSRG-03 (3)

For the isolation of compound LSRG-03 (**3**) the mass of fractions K101 and K102 obtained from first silica gel column K100 were determined to be 178.5 mg. They were further separated by CC over silica gel. An amount of 21 g of dry silica gel were mixed with the eluent consisting of PE/EtOAc (90:10) and filled in the column. When the column bed was settled, the sample was transferred onto the stationary phase. The same solvent mixture was used for the first 100 mL of eluent, then the gradient for 100 mL-steps was changed in 15% steps until composition reached pure EtOAc. Then, a 10% step-wise gradient of EtOAc/MeOH was used in 100 mL steps until a ratio of 70:30 EtOAc/MeOH was reached. Afterwards was the column rinsed with 100 mL pure MeOH. In total, 23 fractions could be obtained. Because of its chromatogram shown in Figure 11 fraction VL5 was weighed (2.5mg) and its purity was additionally checked by TLC. The fraction was defined as LSRG-03 (**3**) and a full NMR spectra set was recorded.

3.2.4 Isolation of LSRG-04 (4)

The silica gel column K200 obtained another interesting fraction: K201 with a dry weight of 23.7 mg. The fraction resuspended in a small amount of MeOH and applied on a sephadex LH20 column (S200). The column was again eluted with MeOH and afforded 13 fractions. Fractions S202 and S203 were combined, TLC was conducted and their mass was determined. Since its purity level was not yet satisfactory for NMR and mass analysis. As a result, fractions S205 and S206 were added and prepared for further purification.

With a total weight of 9.8 mg the pooled fractions were carefully transferred on a prep TLC plate (prep DC II). The thin layer chromatography was developed with a mixture of $CHCl_3$/MeOH 95:5 and a second time with a mixture of 90:10 $CHCl_3$/MeOH. The band with the desired compound was scraped off and the substance resolved in methanol. The silica gel was filtered off using a G5 frit and the substance dried and weighted (2.3 mg). The compound was then pure enough for structural analyses by NMR measurements and mass spectrometry. To prepare it for analysis, it was resolved in deuterated methanol, transferred in an NMR tube and a full NMR spectra set was recorded.

3.2.5 Isolation of K415 (5)

As shown in Figure 8, compound K415 (**5**) was isolated from extract C1351. Liquid extraction with the previously described solvents afforded 0.2 g of chloroform extract. The dried extract was dissolved in methanol and fractioned by a silica gel column (K400). This column chromatography was run with a gradient elution, beginning with the equilibration of the column bed with PE. After subjecting the sample, the eluent started with 100 mL of a mixture of PE/EtOAc 90:10. The amount of EtOAc increased for every 100 mL step by 10 %. When 100 % EtOAc was reached, the gradient was changed to EtOAc/MeOH 10:90 and the amount of MeOH increased in 10 % steps until the column was eluted with 100 % methanol. The chromatography afforded 21 fractions of approximately 50 mL of which K415 showed an interesting HPLC profile and UV spectrum. After checking the purity by TLC and HPLC, the fraction was weighted (0.7 mg) and a full NMR spectra set was recorded, as well as a mass spectrum.

3.2.6 Isolation of RUDS42M (6)

For the separation of natural component RUDS42M a different crude extract (D2024) was used. As described in 3.1.2, the extraction involved an additional liquid extraction step with PE/EtOAc and H_2O. The combined liquid extracts were dried under reduced pressure and subjected onto a silica gel column (K600). Therefore, 20 g of silica gel (0.2–0.5 mm) were weighed and filled in the column by batch technique, the column chromatography was run with a gradient eluent of chloroform and methanol. Starting with 100 % $CHCl_3$, the MeOH ratio increased in 5 % steps (100 mL) until a composition of 60:40 $CHCl_3$/MeOH was reached. Afterwards the stationary phase was rinsed with pure methanol.

This separation step afforded 26 fractions of which three contained the desired compound in considerably amount. Fractions K622 and K623 were subsequently combined and weighted, but the yield was too small for further purification. Consequently, fraction K623 was additionally added. With a total amount of 23.9 mg in total, the sample was subjected to CC over sephadex LH20 (S400).

This CC was run isocratic with methanol and its progress was observed by employing an UV detector. In total 31 fractions were collected and analysed by HPLC measurements and TLC. Fractions S426 and S427 showed promising chromatograms and UV spectra. But the total amount of the pooled fractions S426 and S427 of 1.5 mg was too little for ongoing purification. As a consequence, the more impure fractions S423, S424 and S425 were also added. The combined fractions had to undergo more purification and so several eluent mixtures for a separation by prep TLC were tested. None of them separated the desired compound from the impurities, therefore, it was decided to try and separate the small amount of 3.7 mg with a MPLC. Before subjecting the fractions onto the column, a full NMR set was recorded, to at least have an NMR of the non-purified substance.

The fractions were separated by MPLC with a solvent mixture of H_2O/MeOH. Starting with 98:2 H_2O/MeOH, nine fractions were collected and then the methanol ratio was increased to 97:3 and after ten more fractions, to 85:15. Altogether, 25 fractions were collected and analysed by HPLC and TLC, unluckily the aimed substance seemed to have rearranged itself and could not be found in the fractions any more. Therefore, the NMR set recorded prior to the last MPLC separation, was used for structure determination.

3.2.7 Isolation of BU-RG-01, 02, 03 and 04 (7–10)

These compounds were obtained from the crude extract RUD1413lv of *Rudgea raveniana*. The extraction and purification of the compounds BU-RG-01–04 was performed in course of a bachelor thesis.[42]

3.3 Metabolomic profiling

All substances of interest (Table 2) were diluted to various concentrations in H_2O (100 pg μL^{-1}, 10 pg μL^{-1} and 1pg μL^{-1}) and a mass spectrum was generated by LC-MS (Q Exactive HF). Crude plant extracts of several plant species of interest (Table 3) were generated by extracting leaf material with MeOH in an Eppendorf tube. The samples were extracted in an ultrasonic bath for 20 min. The liquid extracts were transferred to another Eppendorf tube each, dried and diluted to the above-mentioned concentrations (100 pg μL^{-1}, 10 pg μL^{-1} and 1pg μL^{-1}). As well as the standard metabolites, the extracts were analysed by LC-MS analysis.

The measurements and data acquisition were performed by the Department of Analytical Chemistry, University of Vienna using Tracefinder software (4.1, Thermofischer). For verification and practice, the obtained mass spectra were also analysed by using the software Skyline 20.1. As described in 2.3.1, first the library was set up by analysing the standard metabolites.

Table 2. Metabolites used for targeted analysis by metabolomic-profiling

number	metabolites	chemical formula
1	isoalstrostine B	$C_{52}H_{60}N_2O_{22}$
2	isoalstrostine C	$C_{51}H_{58}N_2O_{22}$
11	alstrostine A	$C_{44}H_{56}N_2O_{19}$
12	rudgeifoline	$C_{43}H_{54}N_2O_{19}$
13	5α-carboxystrictosidine	$C_{28}H_{34}N_2O_{11}$
14	nauclealomide B	$C_{26}H_{30}N_2O_{10}$
15	nauclealomide C	$C_{26}H_{30}N_2O_{10}$
16	3,14-dihydro angustoline	$C_{20}H_{19}N_3O_2$
17	angustoline	$C_{20}H_{17}N_3O_2$
18	angustine	$C_{20}H_{15}N_3O$
19	strictosidine	$C_{27}H_{34}N_2O_9$
20	strictosidinic acid	$C_{26}H_{32}N_2O_9$
21	lyalosid	$C_{27}H_{30}N_2O_9$
22	lyalosidic acid	$C_{26}H_{28}N_2O_9$
23	deoxostrictosamide	$C_{26}H_{32}N_2O_7$
24	strictosamide	$C_{26}H_{30}N_2O_8$
25	vincosamide	$C_{26}H_{30}N_2O_8$
26	javaniside	$C_{26}H_{30}N_2O_9$
27	10-hydroxy strictosamide	$C_{26}H_{30}N_2O_9$
28	10-hydroxy 3-*epi*-strictosamide	$C_{26}H_{30}N_2O_9$

A so-called transition-list with information about the molecular name and formula as well as the precursors adduct ($[M+H]^+$, $[M+Na]^+$, $[M-H]^-$) was compiled and thereby the specific product ion was determined. The retention time of the compounds as well as the starting point and ending point (peak boundaries) of it were noted. These peak boundaries were used in the analysis of the extract.

Table 3. Crude extracts analysed by metabolomic profiling

extract number	plant species, collection number
LRE01	*Rudgea skutchii*, 211
LRE03	*R. skutchii*
LRE04	*R. laevis*, 2024
LRE05	*R. laevis*, 2026
LRE06	*R. laevis*, 2024
LRE07	*R. laevis*, 2026
LRE08	*R. reducticalyx*, Dwyer1473
LRE09	*R. skutchii*, 1544
LRE11	*R. coriacea* (Spreng.) K. Schum., 177
LRE12	*R. ciliata* (Ruiz & Pav.) Spreng., 28020
LRE13	*R. gardenioides* (Cham.) Müll. Arg., 3920
LRE14	*R. jasminoides* (Cham.) Müll. Arg., 4712
LRE15	*R. stipulacea* (Dc.) Steyerm,
LRE16	*R. recurva* Müll. Arg., 1356
LRE17	*R. longiflora* Benth, 18648
LRE18	*R. parquioides* (Cham.), 339
LRE19	*Notopleura parasitica* (Sw.) Hammel, 1538
LRE20	*N. anmothyrsa* (K. Schum. & Donn. Sm.) C. M. Taylor, 7021001
LRE21	*N. polyphlebia* (Donn. Sm.) C. M. Taylor, 19021001
LRE22	*N. siggersiana* (Standl.) C. M. Taylor, 1484
LRE23	*R. cornifolia*, 210210071
LRE24	*R. cornifolia*, 1368
LRE25	*R. laevis*, D2024
LRE26	*R. raveniana* W.C., 1413
LRE27	*R. cornifolia* (Kunth) Standl, 1529
LRE28	*R. raveniana*, 1420
LRE29	*R. raveniana*, 1749
LRE30	*R. reducticalyx*, 1475
sl_14	*R. skutchii*, 1351 leaf
sl_15	*R. skutchii*, 1351 stem

The obtained MS data of the extracts were imported to the Skyline software and peak extraction was performed. Peaks in the extracts raw data were matched with the

previously generated data of retention time, peak boundaries and product ion. These hits were checked, and the retention time ranges were manually adjusted for some peaks. When all extracts were analysed a report was generated. The report included information like metabolite name, molecular formula, sample name, measured retention time and area. The obtained data allowed comparison of different plant species and their metabolite content.

4 RESULTS

The results of mass spectrometric and NMR spectroscopic analyses are shown in this chapter. The detected molecular ions as well as the carbon and proton signals for each isolated compound are listed in respective tables. The structure elucidation of the isolated compounds and the comparison to similar metabolites of available literature and NMR prediction tools are also described.[43]

4.1 Results of LSRG-01 (1)

Isoalstrostine B was isolated and characterised for the first time in this work. The mass spectra indicated the molecular formula of $C_{52}H_{60}N_2O_{22}$, resulting in a molecular mass of 1064.4 g mol^{-1}. The structure of isoalstrostine B (LSRG-01) (**1**) is shown in Figure 12.

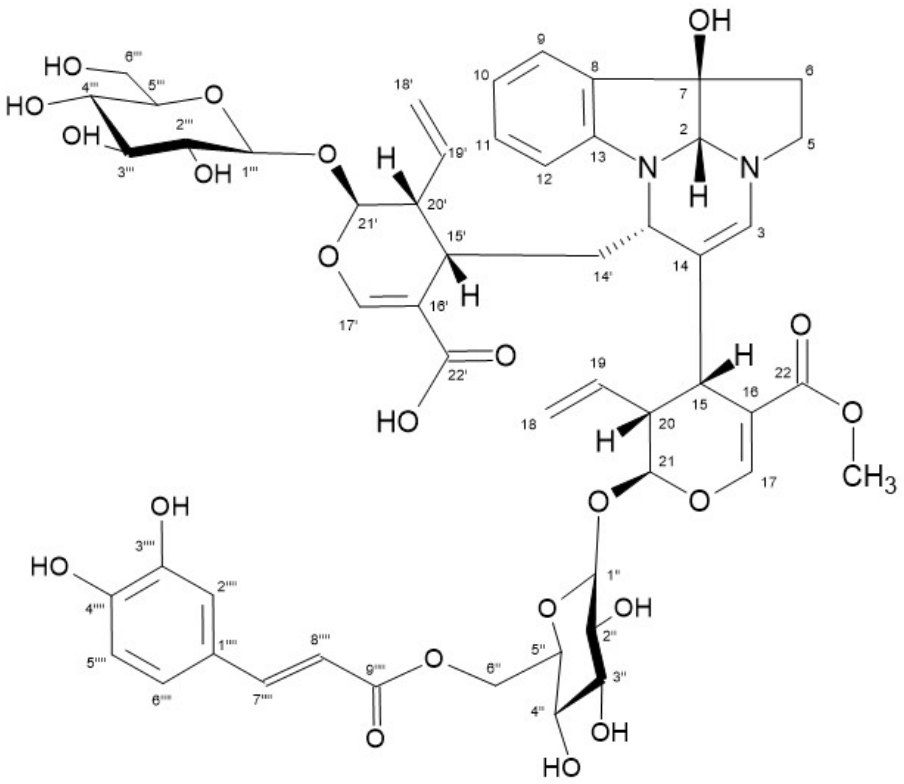

Figure 12. Structure of isoalstrostine B (**1**)

In Table 4 the HR-TOF-ESI-MS data shows the positively and negatively charged molecule ion signals for isoalstrostine B (**1**). The positively, as well as the negatively signal correlated well with the theoretical mass of the molecule.

Table 4. HR-TOF-ESI-MS data: positive and negative mode of isoalstrostine B (**1**) in comparison to the theoretical molecule mass.

molecular ion	m/z meas.	m/z theor.
$[M+Na]^+$	1087.3510	1087.3535
$[M-H]^-$	1063.3583	1063.3559

In alignment with the numbering of carbons in Figure 12, the ^1H NMR and ^{13}C NMR shifts are assigned to their respective position in Table 5. Multiplicity and coupling constant are listed as well.

Table 5. NMR data of isoalstrostine B (**1**) in methanol-d_4. The table shows ^1H NMR shifts (ppm) with the associated integral, multiplicity and coupling constant (Hz) as well as the ^{13}C NMR shifts (ppm)

position	isoalstrostine B (**1**)	
	δ ^1H (ppm)	δ ^{13}C (ppm)
2	4.62 (1H, s)	79.3, d
3	5.61 (1H, s)	133.4, d
5	3.27 (1H, m)	53.7, t
	2.24 (1H, m)	
6	2.28 (1H, m)	36.9, t
	2.15 (1H, m)	
7	-	86.6, s
8	-	133.0, s
9	7.05 (1H, d, 7.15)	125.2, d
10	6.59 (1H, t, 7.15)	119.7, d
11	7.10 (1H, t, 7.15)	130.7, d
12	6.55 (1H, d, 7.15)	110.3, d
13	-	153.2, s
14	-	117.4, s
15	3.22 (1H, m)	37.2, d
16	-	111.7, s
17	7.41 (1H, s)	153.1, d
18	5.15 (1H, d, 17.8)	119.3, t
	5.17 (1H, d,10.73)	
19	5.47 (1H, m)	137.0, d
20	2.51 (1H, m)	47.7, d
21	5.24 (1H, d, 8.05)	97.1, d
22	-	169.0, s
22-O-CH_3	3.62 (3H, s)	51.7, q

position	isoalstrostine B (**1**)	
	δ ^{1}H (ppm)	δ ^{13}C (ppm)
3'	3.97 (1H, d, 12.49)	52.8, d
14'	2.21 (1H, m)	32.7, t
	2.01 (1H, m)	
15'	3.09 (1H, m)	43.8, d
16'	n.d.	n.d.
17'	n.d.	n.d.
18'	5.42 (1H, d, 17.4)	120.3, t
	5.34 (1H, d, 10.73)	
19'	5.82 (1H, m)	135.8, d
20'	2.75 (1H, m)	45.1, d
21'	5.38 (1H, d, 3.58)	98.1, d
22'	n.d.	n.d.
22-OH		
1''	4.66 (1H, d, 8.05)	100.1, d
2''	3.15 (1H, t, 8.05)	75.3, d
3''	3.31 (1H, m)	71.7, d
4''	3.42 (1H, m)	76.2, d
5''	3.26 (1H, m)	77.8, d
6''	4.17 (1H, m)	64.6, t
	4.13 (1H, dd, 5.08, 11.5)	
1'''	4.55 (1H, d, 8.05)	99.7, d
2'''	3.06 (1H, t, 8.05)	74.3, d
3'''	3.22 (1H, m)	77.8, d
4'''	3.21 (1H, m)	71.7, d
5'''	3.20 (1H, m)	78.2, d
6'''	3.81 (1H, dd, 11.57, 1.42)	62.8, t
	3.60 (1H, m)	
1''''	-	127.8, s
2''''	7.06 (1H, s)	115.1, d
3''''	-	146.9, s
4''''	-	149.8, s
5''''	6.82 (1H, d, 8.5)	116.5, d
6''''	6.98 (1H, dd, 8.5, 1.79)	123.4, d
7''''	7.52 (1H, d, 16.1)	146.9, d
8''''	6.18 (1H, d, 16.1)	114.9, d
9''''	-	168.8, s

Isoalstrostine B (**1**) is a newly identified compound and therefore it was essential to determine two more characteristics: the molar decadic constant ε and the optical rotation $[\alpha]_D^{20}$. The values for log ε of the absorption maxima are shown in Table 6, they were calculated using Equation 2.

Table 6. UV/Vis spectroscopy results of isoalstrostine B (**1**) in MeOH. Maxima of Absorption with the regarding Extinction E and ε in L·mol^{-1}·cm^{-1}. Concentration of isoalstrostine B (**1**) [2.49*10^{-6}mol L^{-1}]

UV_{max} (nm)	E	log ε (L·mol^{-1}·cm^{-1})
206	0.8559	5.54
236	0.2061	4.92
302	0.0806	4.51
326	0.0754	4.48

Furthermore, the observed rotation of the polarimeter was converted in the optical rotation by using Equation 3. The optical rotation $[\alpha]_D^{20}$ of isoalstrostine B (**1**) was -1.08°.

4.1.1 Structure elucidation of LSRG-01

1D and 2D NMR measurements of LSRG-01 (**1**) implied a total number of one methyl-, 7 methylene-, 31 methine groups and 10 quaternary carbon atoms. The number of detected carbons deviates by three carbon atoms from the carbons in the molecular formula. This can be explained by non-present signals in the carbon NMR data. The NMR data indicated a tetracyclic ring structure connected to two secoiridoid glucoside units and a caffeic acid attached to a glucose. The location of the first secoiridoid unit was determined with heteronuclear 2D NMR. A $^3J_{H\text{-}C}$ coupling between H-3 and C-15 revealed the connection between C-14 and C-15. The presence of $^3J_{H\text{-}H}$ coupling between C-3', C-14' and C-15' implied the attachment of the second secoiridoid glucose unit to the C-3' of the tetracyclic ring. Signals of H-17', C-17', C-16' and C-22' could not yet be determined due to signal broadening. The location of the caffeic acid could not be assessed via coupling, therefore the carbon and hydrogen shifts were compared to similar structures in other publications and NMR prediction programs.[44, 43] Compounds 1 and 6 of Berger et al., (2015) differed in their shifts of H-6' of the glucose. For compound 1 they are 3.70 (1H, m, H-6a'), 3.60 (1H, m, H-6b'). For compound 6 with a (4''-hydroxy-3'',5''-dimethoxy)-cinnamoyl acid attached to the C-6' of the glucose, they are slightly higher [4.69 (1H,m, H-6'a) 4.39 (1H, m, H-6'b)].[44] This, and prediction of several NMR spectra of different binding positions of the caffeic acid, lead to the elucidated structure with the caffeic acid attached to the C-6" of the respective glucose unit.

The stereochemistry of the molecule in positions C-15, C-20, C-2, C-7 and C-2 as well as for C-15', C-20', C-21' was determined by crosspeaks in the NOESY

spectrum as well as comparing the shifts to those of isoalstrostine A in the work of Kornpointner et al., (2020) and alstrostine A in the work of Schinnerl et al., (2012).[9,13] The two glucose units were elucidated by their $^{3}J_{H\text{-}H}$ COSY crosspeaks and $^{3}J_{C\text{-}H}$ HMBC coupling. Also, their shifts and coupling constants were compared to those of glucose units in similar structures.[13,44]

4.2 Results of LSRG-02 (2)

As isoalstrostine B (**1**), its chemically related compound, isoalstrostine C (**2**) could also be isolated for the first time in this work. The mass spectra indicated the molecular formula of $C_{51}H_{58}N_2O_{22}$, resulting in a molecular mass of 1050.3 g mol^{-1}. The three-dimensional structure of isoalstrostine C (LSRG-02) (**2**) is shown in Figure 13.

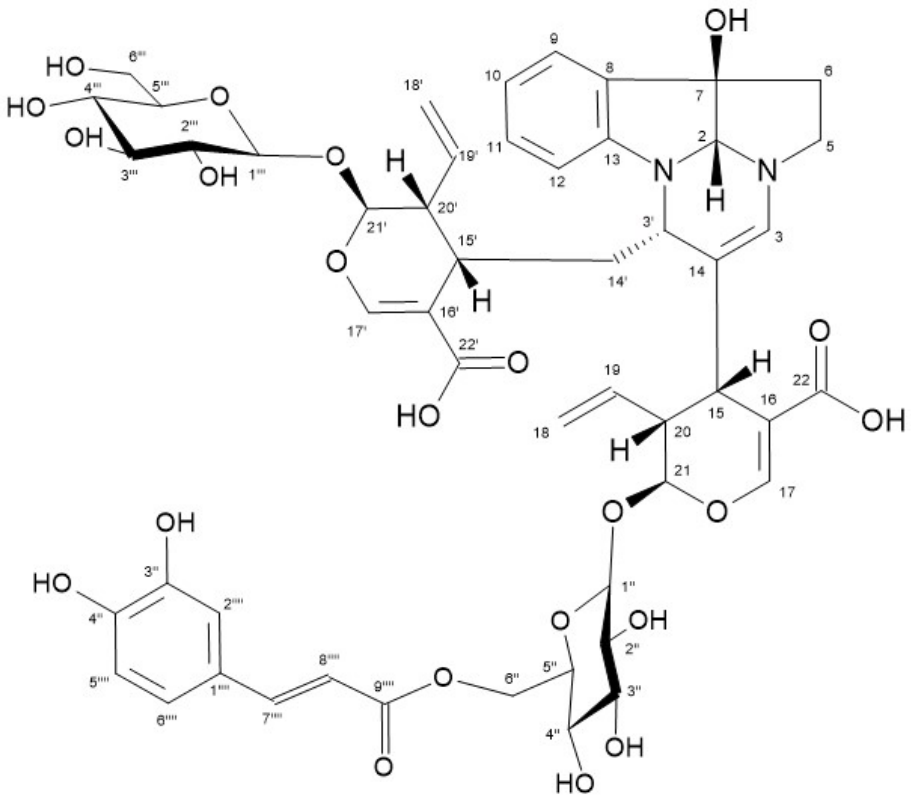

Figure 13. Structure of isoalstrostine C (**2**)

The HR-TOF-MS data of the second compound, isoalstrostine C (**2**) is shown in the following table. It shows the molecular ion in positive and negative mode. (Table 7)

Table 7. HR-TOF-ESI-MS data of isoalstrostine C (**2**)

molecular ion	m/z meas.	m/z theor.
$[M+Na]^+$	1073.3329	1073.3379
$[M-H]^-$	1049.3413	1049.3400

The assignment of each carbon position to the ^1H NMR and ^{13}C NMR shifts are depicted in Table 8. The numbering is according to Figure 13.

Table 8. NMR data of isoalstrostine C (**2**) in methanol-d_4. The table shows ^1H NMR shifts (ppm) with the associated integral, multiplicity and coupling constant (Hz) as well as the ^{13}C NMR shifts (ppm)

position	isoalstrostine C (**2**)	
	δ ^1H (ppm)	δ ^{13}C (ppm)
2	4.64 (1H, s)	79.2, d
3	5.65 (1H, s)	134.9, d
5	3.26 (1H, m)	53.5, t
	2.24 (1H, m)	
6	2.16 (1H, m)	36.7, t
	2.28 (1H, m)	
7	-	86.3, s
8	-	133.1, s
9	7.05 (1H, d, 7.09)	125.1, d
10	6.57 (1H, t, 7.09)	119.5, d
11	7.09 (1H, t, 7.09)	130.6, d
12	6.51 (1H, d, 7.09)	110.2, d
13	-	153.3, s
14	-	118.7, s
15	3.27 (1H, m)	37.1, d
16	n.d.	n.d.
17	n.d.	n.d.
18	5.11 (1H, m)	118.8, t
	5.16 (1H, m)	
19	5.51 (1H, m)	137.0, d
20	2.50 (1H, m)	47.4, d
21	5.24 (1H, d, 7.73)	96.7, d
22	n.d.	n.d.
22-OH	-	-
3'	3.95 (1H, m)	53.1, d
14'	2.00 (1H, m)	32.8, t
	2.11 (1H, m)	
15'	3.03 (1H, m)	44.0, d
16'	n.d.	n.d.
17'	n.d.	n.d.
18'	5.40 (1H, d, 17.34)	120.0, t

position	isoalstrostine C (**2**)	
	δ ^{1}H (ppm)	δ ^{13}C (ppm)
	5.33 (1H, d, 10.95)	
19'	5.83 (1H, m)	136.3, d
20'	2.72 (1H, m)	45.3, d
21'	5.36 (1H, d, 3.68)	98.2, d
22'	n.d.	n.d.
22-OH		
1''	4.66 (1H, d, 7.73)	100.4, d
2''	3.17 (1H, m)	74.7, d
3''	3.42 (1H, m)	71.2, d
4''	3,44 (1H, m)	76.1, d
5''	3.41 (1H, m)	78.3, d
6''	4.20 (1H, dd, 11.59, 4.51)	64.9, t
	4.14 (1H, d, 4.51)	
1'''	4.56 (1H, d, 7.73)	99.8, d
2'''	3.08(1H, t, 7.73)	74.4, d
3'''	3.30 (1H, m)	77.8, d
4'''	3.21 (1H, m)	71.4, d
5'''	3.22 (1H, m)	77.9, d
6'''	3.81 (1H, d, 11.59)	62.7, t
	3.61 (1H, m)	
1''''	-	127.6, s
2''''	7.08 (1H, s)	115.2, d
3''''	-	146.9, s
4''''	-	149.7, s
5''''	6.82 (1H, d, 8.37)	116.6, d
6''''	6.97 (1H, dd, 8.37, 1.93)	123.1, d
7''''	7.53 (1H, d, 16.02)	147.0, d
8''''	6.20 (1H, d, 16.02)	114.9, d
9''''	-	169.0, s

As compound **1**, isoalstrostine C (**2**) was also a newly identified natural component. Therefore, the extinction at its UV maxima was determined and the molar decadic extinction coefficient was calculated with Equation 2. (Table 9)

Table 9. UV/Vis spectroscopy results of isoalstrostine C (**2**) in MeOH. Maxima of Absorption with the regarding Extinction E and ε in L·mol^{-1}·cm^{-1}. Concentration of isoalstrostine C (**2**) [1.52*10^{-7} mol L^{-1}]

UV_{max} (nm)	E	log ε (L·mol^{-1}·cm^{-1})
206	0.0502	5.52
236	0.0571	5.57
302	0.1557	6.01
326	1.1373	6.87

Additionally, the optical rotation was calculated. The observed value of the polarimeter was converted using Equation 3. The optical rotation $[\alpha]_D^{20}$ of isoalstrostine C (**2**) was -1.01°.

4.2.1 Structure elucidation of LSRG-02 (2)

For LSRG-02 (**2**), a total number of seven methylene-, 30 methine groups and eight quaternary carbon atoms were identified. It showed the same coupling between the tetracyclic ring and the two secoiridoid glucose units as LSRG-01 (**1**). As for LSRG-01 (**1**), for LSRG-02 (**2**) the atoms H-17', C-17', C-16' and C-22' could not yet be determined. Additionally, the same problem was observed for H-17, C-17, C-16 and C-22. The difference of the two compounds lied exactly in this part of the molecule: where LSRG-01 (**1**) had an ester attached at C-16, compound **2** was characterised by a second acid moiety.

In the second secoiridoid unit, they both showed an acid unit and no NMR data for the atoms H-17', C-17', C-16' and C-22'. In the first unit, compound **1** characterised by an ester, which led to no loss of data, compound **2** however characterised by another acid unit and shows no NMR data for the atoms. This led to the assumption, that the acid unit may be responsible for the lowering and therefore loss of signal intensity (high) for the adjacent atoms.

The stereochemistry was determined as already mentioned for isoalstrostine B in 4.1.1. The higher shifts of C-21 and C-21' indicated the attachment of the respective ß-D-glucose. The NOESY crosspeak between C-21 and H-1'' as well as C-21' and H-1''' confirmed the bonds.

4.3 Results of LSRG-03

7-*O*-Butylsecologanic acid (LSRG-03) (**3**) was also isolated from extract AB1351. The data from mass measurements resulted in the molecular formula of $C_{20}H_{30}O_{10}$ with the molecular mass of 430.5 g mol^{-1}. The structure is shown in Figure 14.

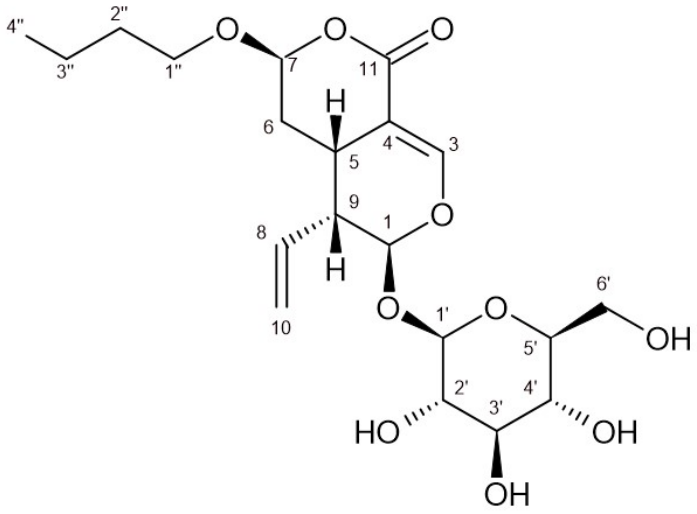

Figure 14. Structure of 7-*O*-butylsecologanic acid (**3**)

The molecular ion in positive mode for LSRG-03 (**3**) is shown in Table 10. It correlated with the theoretical mass of 7-*O*-butylsecologanic acid.

Table 10. HR-TOF-ESI-MS data of 7-*O*-butylsecologanic acid (**3**)

molecular ion	m/z_{gem}	$m/z_{theor.}$
$[M+Na]^+$	453.1738	453.1737

In Table 11 the ^{1}H NMR and ^{13}C NMR shifts are assigned to its carbon position according to Figure 14. The coupling constant and multiplicity are also given.

Table 11. NMR data of 7-*O*-butylsecologanic acid (**3**) in methanol-d_4. The table shows ^{1}H NMR shifts (ppm) with the associated integral, multiplicity and coupling constant (Hz) as well as the ^{13}C NMR shifts (ppm)

position	7-*O*-butylsecologanic acid (**3**)	
	δ ^{1}H (ppm)	δ ^{13}C (ppm)
1	5.55 (1H, d, 1.76)	98.7, d
3	7.60 (1H, d, 2.41)	154.44, d
4	-	105.4, s
5	3.36 (1H, m)	22.9, d
6	1.85 (1H, dd, 13.57, 4.88)	30.4, t
	1.72 (1H,dd 13.57, 2.71)	
7	5.44 (1H, t, 2.44)	102.3, d
8	5.53 (1H, d, 1.76)	133.5, d
9	2.66 (1H, m)	43.7, d
10	5.32 (1H, d, 1.76)	121.0, t
	5.28 (1H, dd, 1.76)	
11	-	167.8, s
1'	4.69 (1H, d, 7.87)	100.5, d
2'	3.20 (1H, t, 7.87)	74.6, d
3'	3.32 (1H, m)	78.4, d
4'	3.29 (1H, m)	71.4, d
5'	3.34 (1H, m)	78.1, d
6'	3.66 (1H, m)	62.6, t
	3.88 (1H, dd, 12.21, 2.44)	
1''	3.84 (1H, m)	70.4, t
	3.61 (1H, m)	
2''	1.37 (1H, m)	20.2, t
3''	1.58 (1H, m)	32.6, t
4''	0.92 (3H, t, 7.06)	14.1, q

4.3.1 Structure elucidation of LSRG-03 (3)

In mass analysis the molecule ion $[M+Na]^+$ of 453.1738 was determined in positive mode. It corresponds with the theoretical *m/z* 453.1737 of the molecular formula of $C_{20}H_{30}O_{10}Na$ very well.

The interpretation of 2D NMR spectra resulted in a total number of one methyl-, six methylene-, 11 methine groups and two quaternary carbon atoms. Exact structure elucidation of LSRG-03 (**3**) ended in the identification of the natural component 7-*O*-butyl-secologanic acid.[45]

$^3J_{H\text{-}H}$ COSY crosspeaks allowed the characterization of the butyl-group. The terminal methyl group C-4'', the three methylene-groups C-3'', C-2'' and C-1'' were determined. The C-1'' proton showed higher shifts due to its neighbourhood to an

oxygen. A secluded spin system of C-1'' to C-4'' in the TOCSY spectrum underlined the presence of the *O*-butyl-group.

The bond of the butyl-group to the iridoid core structure was directed by $^{3}J_{H\text{-}C}$ coupling in HMBC between C-7 and H-1''. Additionally, H-7 showed coupling in $^{3}J_{H\text{-}C}$ coupling to the quaternary carbon C-11. Another $^{3}J_{H\text{-}C}$ -coupling was observed between C-11 and H-3. The connection of C-4 and C-5 was given by the HMBC signals between H-3 and H-5. The HMBC and COSY signals of H-5 to H-6 and C-7 completed the first ring structure. The second ring closure and therefore iridoid structure was indicated by the $^{3}J_{H\text{-}H}$ COSY crosspeaks between H-5 and H-9, H-9 and H-1, as well as the HMBC signals between C-1 and H-3. The HMBC and COSY crosspeaks of position 8, 9 and 10 allowed the connection between C-9 and the double bond of C-8 and C-10. This attachment concluded the iridoid ring structure.

The attachment of the glucose moiety was determined by the HMBC-crosspeak between C-1 and H-1'. The position of the methine and methylene groups was determined by the $^{3}J_{H\text{-}H}$ COSY signals as well as comparing the proton and carbon shifts with other glycosylated natural components.[45,44]

The stereochemistry was determined by the NOESY crosspeaks between H-9 and H-5 as well as H-1 and H-1'. The stereochemistry of C-7 was confirmed by the missing NOESY crosspeak between H-7 and H-5 as well comparing the NMR shifts and coupling constants with compound *epi*-vogeloside.[46]

4.4 Results of LSRG-04 (4)

The isolated compound LSRG-04 (**4**) was the already known *epi*-vogeloside. The structure of the natural component is shown in Figure 15. The determined molecular mass was 388.4 g mol^{-1}, resulting in a molecular formula of $C_{17}H_{24}O_{10}$.

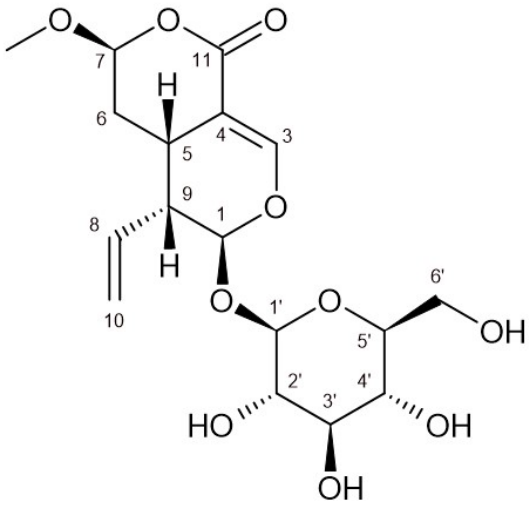

Figure 15. Structure of *epi*-vogeloside (**4**)

The HR-TOF-ESI-MS data provided a molecular ion peak $[M+Na]^+$ in positive mode. The measured molecular mass correlated well with the theoretical mass. (Table 12)

Table 12. HR-TOF-ESI-MS data of *epi*-vogeloside (**4**)

molecular ion	m/z_{gem}	$m/z_{theor.}$
$[M+Na]^+$	411.1295	411.1267

The assignment of the ^1H NMR and ^{13}C NMR peaks are shown in Table 13. It correlates with the numbering in Figure 15.

Table 13. NMR data of *epi*-vogeloside (4) in methanol-d_4. The table shows ^{1}H NMR shifts (ppm) with the associated integral, multiplicity and coupling constant (Hz) as well as the ^{13}C NMR shifts (ppm)

position	*epi*-vogeloside (**4**)	
	δ ^{1}H (ppm)	δ ^{13}C (ppm)
1	5.55 (1H, d, 1.64)	98.6, d
3	7.62 (1H, d, 2.67)	154.5, d
4	-	105.1, s
5	3.36 (1H, m)	22.83, d
6	1.71 (1H, dt, 13.36, 2.46)	30.2, t
	1.86 (1H, m)	
7	5.33 (1H, t, 2.46)	103.3, d
7-OCH_3	3.51 (3H, s)	56.9, q
8	5.53 (1H, dd, 6.98, 3.67)	133.0, d
9	2.65 (1H, m)	43.6, d
10	5.31 (1H, m)	121.0, t
	5.27 (1H, t, 2.26)	
11	-	167.5, s
1'	4.68 (1H, d, 7.8)	100.4, d
2'	3.19 (1H, dd, 7.8, 1.2)	74.6, d
3'	3.35 (1H, m)	78.1, d
4'	3.28 (1H, m)	71.5, d
5'	3.31 (1H, m)	78.4, d
6'	3.65 (1H, m)	62.54, t
	3.88 (1H, dd, 11.50, 2.05)	

4.4.1 Structure elucidation of LSRG-04

Compound LSRG-04 (**4**) had the same iridoid core structure as LSRG-03 (**3**). All together the elucidation resulted in one methyl-, three methylene-, 11 methine groups and two quaternary carbon atoms. HMBC crosspeaks are observed for C-11 and H-3, C-11 and H-7. The position of H-1 is directed by a $^{3}J_{H\text{-}C}$ crosspeak with C-3. $^{3}J_{H\text{-}H}$ COSY signals were determined for H-9 and H-5 as well as for H-5 and H-6. The coupling of H-6 and H-7 concluded the first ring closure.

The attachment of the glucose moiety was again at position 1, confirmed by $^{3}J_{H\text{-}C}$ HMBC crosspeak between H-1 and C-1'. The proton and carbon positions of the glucose were determined by comparing ^{1}H and ^{13}C NMR shifts with the work of Berger et al., (2017) and Tomassini et al., (1995).[45,47] Furthermore, the COSY crosspeaks and TOCSY spin system were taken into consideration.

The HMBC crosspeak between H-8 and C-9 confirmed the attachment of the double bond which was determined by the $^{3}J_{H\text{-}H}$ COSY crosspeaks between H-8 and H-10. Another $^{3}J_{H\text{-}C}$ HMBC signal confirmed the methyl group attached to C-7.

The stereochemistry of the natural component was determined by comparing the data with published paper Recio-Iglesias et al., (1992).[46] Because of the proton shifts and coupling constants, the compound was determined to be the epimer of vogeloside, *epi*-vogeloside. Additionally, the 3D structure was confirmed by NOESY data. The crosspeak between H-9 and H-5, H-9 and H-8 and the missing crosspeak between H-5 and H-7 proved the *epi*-vogeloside structure. The ß-D-glucose was determined by the NOESY crosspeak between H-1 and H-1'.

The structure elucidation concluded with the structure given in Figure 15, a known natural component, *epi*-vogeloside. The corresponding molecular formula is $C_{17}H_{24}O_{10}$ with a molecular mass of 388.14 g mol^{-1}. The mass matched with the molecular ion peak $[M+Na]^{+}$ with a *m/z* of 411.1267 g mol^{-1} and confirmed the structure elucidation.

4.5 Results of BU-RG-01

Mass analysis confirmed the molecular mass of 430.5 g mol^{-1}, resulting with the molecular formula $C_{20}H_{30}O_{10}$. The natural component was as for LSRG-03 (**3**) 7-*O*-butylsecologanic acid. The structure of the known natural component is shown in Figure 16.

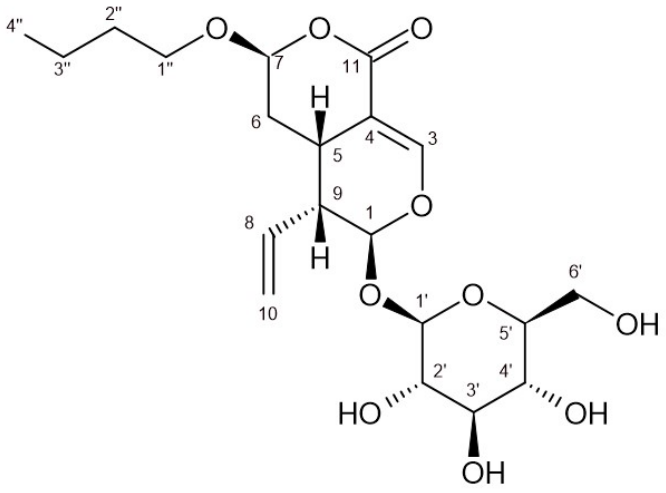

Figure 16. Structure of 7-*O*-butylsecologanic acid (**7**)

Mass analysis resulted in molecular ion peaks in positive and negative mode. The measured *m/z* ratios correlated with the theoretical mass of 7-*O*-butylsecologanic acid. The molecular ions for positive and negative mode are depicted in Table 14.

Table 14. HR-TOF-ESI-MS data of 7-*O*-butylsecologanic acid (**7**)

molecular ion	m/z meas.	m/z theor.
$[M+Na]^+$	453.1698	453.1737
$[2M+Na]^+$	883,3490	883.3575
$[2M-H]^-$	859.3645	859.3600

The peaks of ^1H NMR and ^{13}C NMR are assigned to the carbon positions in Table 15. The numbering is shown in Figure 16.

Table 15. NMR data of 7-*O*-butylsecologanic acid (**7**) in methanol-d_4. The table shows ^1H NMR shifts (ppm) with the associated integral, multiplicity and coupling constant (Hz) as well as the ^{13}C NMR shifts (ppm)

position	7-*O*-butylsecologanic acid (**7**)	
	δ ^1H (ppm)	δ ^{13}C (ppm)
1	5.56 (1H, d, 5.64)	98.9, d
3	7.62 (1H, s)	154.5, d
4	-	105.4, s
5	3.38 (1H, m)	23.2, d
6	1.72 (1H, t, 13.91)	30.4, t
	1.85 (1H, dd, 13.91, 5.01)	
7	5.44 (1H, d, 6.45)	102.6, d
8	5.53 (1H, t, 9.68)	133.2, d
9	2.67 (1H, m)	43.4, d
10	5.31 (1H, d, 8.06)	121.7, t
	5.26 (1H, d, 8.06)	
11	-	167.7, s
1'	4.68 (1H, d, 7.26)	100.5, d
2'	3.21 (1H, t, 8.06)	74.6, d
3'	3.31 (1H, m)	78.7, d
4'	3.29 (1H, m)	71.4, d
5'	3.35 (1H, m)	78.4, d
6'	3.67 (1H, m)	63.7, t
	3.88 (1H, m)	
1''	3.87 (1H, m)	71.5, t
	3.62 (1H, m)	
2''	1.59 (1H, m)	33.3, t
3''	1.39 (2H, m)	21.2, t
4''	0.94 (3H, t, 7.56)	15.2, q

4.5.1 Structure elucidation of BU-RG-01

Compound BU-RG-01 (**7**) was the same as LSRG-03 (**3**), 7-*O*-butylsecologanic acid. The structure elucidation is described in chapter 4.3.1. The attachment of the *O*-butyl-group was determined by the $^{3}J_{H\text{-}C}$ HMBC crosspeak between C-1'' and H-7. The stereochemistry of C-7 was again confirmed by the NOESY crosspeaks and by comparing the coupling constants, with the work of Recio-Iglesias et al., (1992) and Tomassini et al., (1995).[45,46]

4.6 Results of BU-RG-02

As for LSRG-04, the interpretation of the NMR data of analyte BU-RG-02 resulted in the structure of natural component *epi*-vogeloside (**8**). The chemical structure with a molecular formula of $C_{17}H_{24}O_{10}$ and a molecular mass of 388.4 g mol^{-1} is shown in Figure 17.

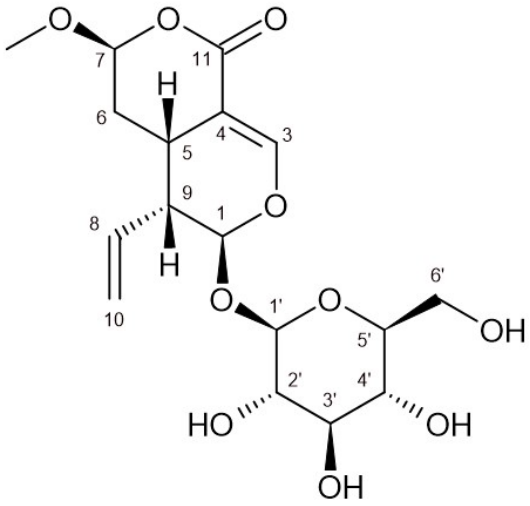

Figure 17. Structure of *epi*-vogeloside (**8**)

The mass analysis resulted in two molecular ions in positive and two in negative mode. (Table 16) All four corresponded to the molecular mass of 388.4 g mol^{-1}.

Table 16. HR-TOF-ESI-MS data of *epi*-vogeloside (**8**)

molecular ion	*m/z* meas.	*m/z* theor.
$[M+Na]^+$	411.1238	411.1267
$[2M+Na]^+$	799.2574	799.2637
$[2M-H]^-$	775.2691	775.2661
$[M+FA-H]^-$	433.1368	433.1346

A list of all chemical shifts for ^{1}H NMR, ^{13}C NMR as well as the associated integral, coupling constant and multiplicity are listed in Table 17. The spectrum was recorded in methanol-d_4.

Table 17. NMR data of *epi*-vogeloside (**8**) in methanol-d_4. The table shows ^{1}H NMR shifts (ppm) with the associated integral, multiplicity and coupling constant (Hz) as well as the ^{13}C NMR shifts (ppm)

position	*epi*-vogeloside (**8**)	
	δ ^{1}H (ppm)	δ ^{13}C (ppm)
1	5.54 (1H, d, 7.63)	98.6, d
3	7.62 (1H, d, 2.29)	154.4, d
4	-	105.1, s
5	3.37 (1H, m)	23.2, d
6	1.86 (1H, dd, 4.72, 13.57)	30.4, t
	1.73 (1H, dd, 2.95, 13.57)	
7	5.36 (1H, m)	103.0, s
8	5.51 (1H, t, 9.44)	133.5, d
9	2.64 (1H, m)	43.7, d
10	5.33 (1H, d, 5.90)	121.08, t
	5.26 (1H, d, 11.21)	
11	-	167.7, s
7-OCH_3	3.52 (3H, s)	56.8, q
1''	4.68 (1H, d, 7.50)	100.4, d
2''	3.19 (1H, t, 8.26)	74.7, d
3''	3.36 (1H, m)	78.8, d
4''	3.28 (1H, m)	71.4, d
5''	3.31 (1H, m)	78.3, d
6''	3.66 (1H, m)	62.3, t
	3.88 (1H, d, 12.39)	

4.6.1 Structure elucidation of BU-RG-02

The structure elucidation for *epi*-vogeloside is already described in chapter 4.4.1. Compound BU-RG-02 showed the same NOESY crosspeaks and similar shifts as well as coupling and was consequently also recognized as *epi*-vogeloside.

4.7 Results of BU-RG-03

The structure elucidation of BU-RG-03 (**9**) was complicated because it was a mixture of two or more natural products. One of the metabolites could be determined to be sweroside (**9**). The relevant structure is shown in Figure 18. The molecular mass for this natural component was 358.1 g mol^{-1} and the molecular formula $C_{16}H_{22}O_9$.

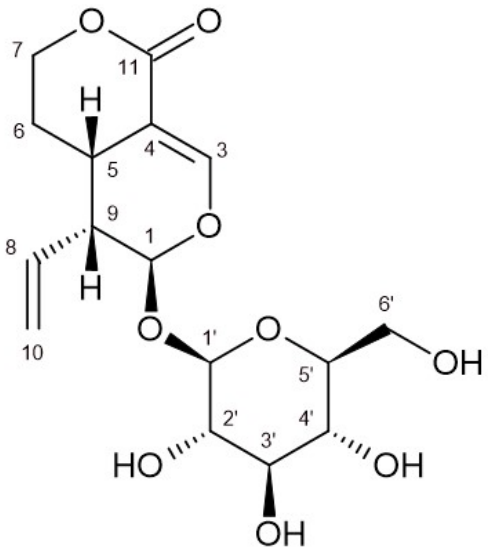

Figure 18. Structure of sweroside (**9**)

The HR-TOF-MS data was not clear and there was no molecular ion peak representing the mass of sweroside (**9**). The structure elucidation relied solely on the 1D and 2D proton and carbon NMR data. The assignment of the NMR shifts is listed in Table 18, the numbering relies on the structure depicted in Figure 18.

Table 18. NMR data of sweroside (**9**) in methanol-d_4. The table shows ^{1}H NMR shifts (ppm) with the associated integral, multiplicity and coupling constant (Hz) as well as the ^{13}C NMR shifts (ppm)

position	sweroside (**9**)	
	δ ^{1}H (ppm)	δ ^{13}C (ppm)
1	5.56 (1H, d, 5.41)	98.0, d
3	7.60 (1H, dd, 12.27, 2.46)	154.6 , d
4	-	105.0, s
5	3.18 (1H, m)	28.6, d
6	1.71 (1H, t, 13.11)	26.1, t
	1.78 (1H, d, 13.11)	
7	4.37 (1H, dt, 13.11, 2.30)	69.7, t
	4.47 (1H, d, 13.11)	
8	5.53 (1H, m)	133.0, d
9	2.71 (1H, m)	43.9, d
10	5.32 (1H, m)	120.8, t
	5.24 (1H, m)	
11	-	167.3, s
1'	4.69 (1H, d, 7.87)	100.3, d
2'	3.19 (1H, m)	74.6, d
3'	3.31 (1H, m)	79.2, d
4'	3.28 (1H, m)	71.7, d
5'	3.36 (1H, m)	78.3, d
6'	3.66 (1H, m)	62.7, t
	3.89 (1H, d, 11.40)	

4.7.1 Structure elucidation of BU-RG-03

NMR based structure elucidation resulted in a molecule assembled by 4 methylene-, 10 methine groups and 2 quaternary carbon atoms, with the structure shown in Figure 18. C-7 showed a higher shift due to its neighbourhood to an oxygen. $^{3}J_{H\text{-}H}$ COSY coupling determined the bond between C-6 and C-7. The linkage of C-6 to C-1 over C-5 and C-9 was also determined by COSY crosspeaks between the neighbouring protons. The position of C-4 and C-3 was confirmed by HMBC coupling between H-9 and C-4, C-4 and H-3, as well as H-3 and C-1. C-11 showed crosspeaks in the HMBC spectrum with H-7 and H-3.

The attachment of the glucose moiety was determined by the HMBC crosspeak between C-1 and H-1'. $^{3}J_{H\text{-}H}$ COSY crosspeaks and TOCSY spin system were taken into consideration to determine the proton and carbon positions of the glucose. Furthermore, the ^{1}H and ^{13}C NMR shifts were compared with the work of Berger et al., (2017), and Tomassini et al., (1995).[45,47]

The three dimensional structure was confirmed by NOESY data by the crosspeak between H-9 and H-5, H-9 and H-8. The ß-D-glucose was determined by the NOESY crosspeak between H-1 and H-1' as well as comparing the shifts and coupling constants with the work of Berger et al., (2015).[44]

4.8 Results of BU-RG-04

The fourth compound isolated from extract RUD1413lv turned out to be secologanin dibutylacetal. The chemical structure with a molecular formula of $C_{25}H_{42}O_{11}$ and a molecular mass of 518.6 g mol^{-1} is shown in Figure 17.

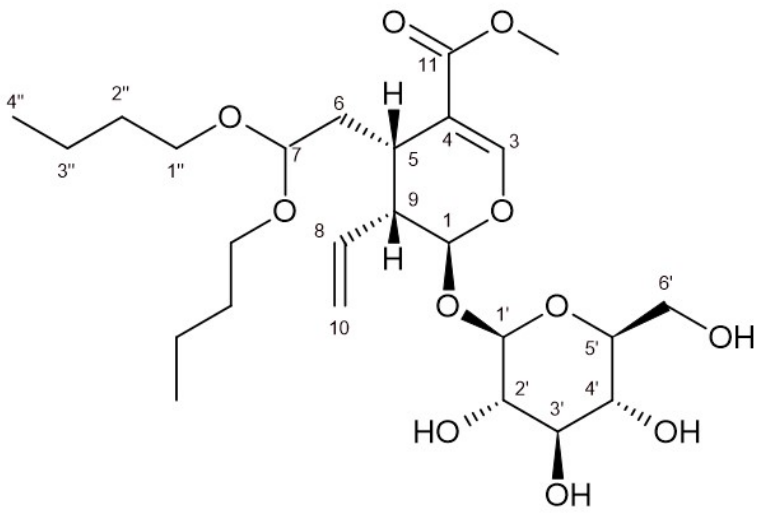

Figure 19. Structure of secologanin dibutylacetal (**10**)

Mass analysis resulted in molecular ion peaks in positive and negative mode. The measured *m/z* ratios correlated with the theoretical mass of secologanin dibutylacetal. The molecular ions for positive and negative mode are depicted in Table 19.

Table 19. HR-TOF-ESI-MS data of secologanin dibutylacetal (**10**)

molecular ion	*m/z* meas.	*m/z* theor.
$[M+Na]^+$	541.2585	541.2625
$[2M+Na]^+$	1059.5254	1059.5352
$[2M-H]^-$	1035.5408	1035.5376
$[M+FA-H]^-$	563.2725	563.2704

Consistent with the numbering of carbons in Figure 12, the ^{1}H NMR and ^{13}C NMR shifts are assigned to their respective position in Table 20.

Table 20. NMR data of secologanin dibutylacetal (**10**) in methanol-*d*$_4$. The table shows ^{1}H NMR shifts (ppm) with the associated integral, multiplicity and coupling constant (Hz) as well as the ^{13}C NMR shifts (ppm)

position	secologanin dibutylacetal (**10**)	
	δ ^{1}H (ppm)	δ ^{13}C (ppm)
1	5.50 (1H, d, 5.09)	97.7, d
3	7.42 (1H, d, 1.03)	153.0, d
4	-	112.4, s
5	2.97 (1H, dd, 6.36, 12.73)	29.1, d
6	2.10 (1H, m)	33.6, t
	1.63 (1H, m)	
7	4.61 (1H, t, 5.46)	103.1, d
8	5.74 (1H, m)	135.2, d
9	2.68 (1H, m)	45.8, d
10	5.31 (1H, d,16.54)	119.3, t
	5.26 (1H, d, 10.82)	
11	-	169.3, s
11-OCH_3	3.69 (3H, s)	52.3, t
1'	4.67 (1H, d, 7.0)	100.2, d
2'	3.19 (1H, t, 8.27)	74.5, d
3'	3.35 (1H, t, 3.82)	77.8, d
4'	3.27 (1H, t, 9.54)	71.3, d
5'	3.28 (1H, m)	78.4, d
6'	3.66 (1H, dd, 5.73, 12.09)	62.1, t
	3.90 (11H, d, 12.09)	
1''	3.41 (1H, m)	66.2, t
	3.61 (1H, m)	
	3.42 (1H, m)	67.6, t
	3.58 (1H, m)	
2''	1.54 (1H, m)	33.2, t
3''	1.39 (1H, m)	20.9, t
4''	0.94 (3H, s)	14.6, q

4.8.1 Structure elucidation of BU-RG-04

The structural analysis of BU-RG-04 resulted in two methyl-, nine methylene-, 11 methine groups and two quaternary carbon atoms. In mass analysis the molecule ion $[M+Na]^+$ of 541.2585 g mol^{-1} as well as $[2M+Na]^+$ with a mass of 1059.5254 g mol^{-1} was determined in positive mode. In negative mode the molecule ions $[2M-H]^-$ and $[M+FA-H]^-$ with masses of 1035.5408 and 563.2725 g mol^{-1} were detected. The measured *m/z*

corresponded well to the theoretical mass of secologanin dibutylacetal (518.6 g mol^{-1}) with a molecular formula of $C_{25}H_{42}O_{11}$.

The attachment of the glucose moiety was again at position 1, confirmed by $^{3}J_{H-C}$ HMBC crosspeak between H-1 and C-1'. The proton and carbon positions of the glucose were determined by comparing ^{1}H and ^{13}C NMR shifts with the work of Berger et al., 2017.[47] Furthermore, the COSY crosspeaks and TOCSY spin system were taken into consideration.

The HMBC crosspeak between H-8 and C-9 confirmed the attachment of the double bond which was determined by the $^{3}J_{H-H}$ COSY crosspeaks between H-8 and H-10. Another $^{3}J_{H-C}$ HMBC signal confirmed the methyl group attached to C-7.

TOCSY spectra showed a spin system for protons H-1''– H-4'', indicating the butyl-group, $^{3}J_{H-H}$ COSY signals confirmed their positions. The chemically equivalent protons of both butyl-groups could not be distinguished and therefore their ^{1}H signals showed double intensity. The neighbourhood of C-1'' to an oxygen resulted in higher proton shifts, the $^{3}J_{H-C}$ HMBC between C-7 and H-1'' connected the butyl-groups with the secoiridoid glycoside.

The secoiridoid moiety had $^{3}J_{H-C}$ HMBC and $^{3}J_{H-H}$ COSY signals similar to those of compounds **1**–**4** and **7**–**10** allowing the characterization of the residual structure. The stereochemistry of C-1, C-5 and C-9 were determined by NOESY crosspeaks.

4.9 Results of K415M

Mass analysis resulted in molecular ion peaks in positive and negative mode. The measured *m/z* ratios correlated with a molecular formula of $C_{10}H_{12}O_4$. The molecular ions for positive and negative mode are depicted in Table 21.

Table 21. HR-TOF-ESI-MS data of K415M (**5**)

molecular ion	$m/z_{meas.}$	$m/z_{theor.}$
$[M+Na]^+$	219.0628	219.0633
$[M-H]^-$	195.0660	195.0658

The NMR data showed three proton signals 6.79, 6.64 and 7.10 suggesting a trisubstituted benzene ring and a methyl group at 3.91 suggesting an -OMe group. The remaining signal was insufficient for further elucidation. Neither the HMBC nor the HSQC offered conclusive information about the molecule. The natural compound must

be further enriched, purified and analysed again to get a better result for the structural elucidation. The obtained signals are shown in Table 22.

Table 22. NMR data of K415M (**5**) in methanol-d_4. The table shows ^{1}H NMR shifts (ppm) as well as the ^{13}C NMR shifts that could be obtained from the NMR spectra.

position	K415M (**5**)	
	δ ^{1}H (ppm)	δ ^{13}C (ppm)
1	3.91	56.5
3	6.87	116.2
4	7.56	111.9
5	7.57	124.7

4.10 Results of RUDS42M

The UV spectra of compound RUDS42M showed similar UV maxima as the previously described isoalstrostines. The mass would also underline the assumption of an alstrostine derivative. It showed molecular ions suitable for a molecular formula of $C_{53}H_{62}N_2O_{22}$ with a molecular mass of 1078.4 g mol^{-1}. The molecular ion peaks of positive and negative mode are listed in Table 23. The estimated structure is depicted in Figure 20.

Table 23. HR-TOF-ESI-MS data of RUDS42M (**6**)

molecular ion	m/z meas.	m/z theor.
$[M+Na]^+$	1101.3629	1101.3691
$[M-H]^-$	1077.3745	1077.3716

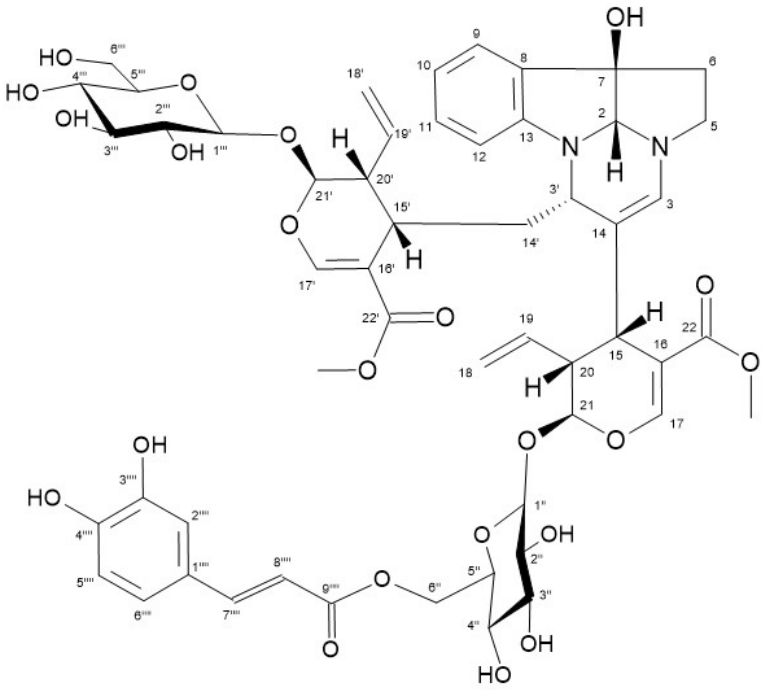

Figure 20. Assumed structure of RUDS42M (**6**). The structure could not be elucidated due to inadequate NMR data.

The molecular formula could correspond to an isoalstrostine with two ester units in the secoiridoid parts. The structure elucidation by NMR data was difficult. The impurities predominated the signals of compound 6. Single one-dimensional carbon and proton signals were recognized, but not enough to construct a carbon skeleton for the assumed metabolite. The two-dimensional NMR data showed only restricted crosspeaks for proton and carbon coupling and therefore could not connect proton and carbons for a molecular structure.

As described in 3.2.6, it was aspired to further purify the natural component to get enhanced NMR spectra. The purification process did not work and therefore prevented the successful structure elucidation of RUDS42M (**6**).

4.11 Result of Omics experiments

The simplified results of the profiling and data analysis are shown in Table 24 and Table 25. The tables are divided in two compound groups: Strictosidine and its derivatives (Table 25) and the novel alstrostine group as well as some other natural components (Table 24). A table with all the results is given in the supplement.

Compounds of the alstrostine group have been found in several *Rudgea* species as well as *Notopleura* species. Alstrostine A (**11**) was detected in *Rudgea* species *laevis, reductivalyx, ciliate* and *recurva* as well as in *Neutopleura amythyrsa* and *siggersiana.* The newly isolated and described isoalstrostine B (**1**) was only found in *R. jasminoides*, isoalstrostine C (**2**) only in *R. laevis*. 5α-Carboxystrictosidine (**13**) was the only analyte found in the two crude extracts of *R. skutchii*. Nauclelalimide B (**14**) and C (**15**) could not be differentiated in mass spectrometry, they were found in *R. parquioides.*

Table 24. Simplified results of metabolomic-profiling of methanolic leaf and stem material. Full information about the plant extracts are given in Table 3.

			compound							
genus	species	sample	**1**	**2**	**11**	**13**	**14/15**	**16**	**17**	**18**
Rudgea	*laevis*	2026 (a)		•	•					
	laevis	2024			•					
	laevis	2026 (b)			•					
	reducticalyx	1473			•					
	ciliata	28020			•					
	recurva	1356			•					
	skutchii, leaf	1351				•				
	skutchii, stem	1351				•				
	jasminoides	4712	•							
	parquioides	339					•			
Notopleura	*anmothyrsa*	7021001			•					
	siggersiana	1484			•					

isoalstrostine B (**1**), isoalstrostine C (**2**), alstrostine A (**11**), rudgeifoline (**12**), 5α-carboxystrictosidine (**13**), nauclealomide B (**14**), nauclealomide C (**15**), 3,14-dihydro angustoline (**16**), angustoline (**17**), angustine (**18**). Compound **14** and **15** could not be distinguished due to their identical molecular mass. *R. laevis* 2026 a and b are from the same sampling number but were stored in separate bags.

• analyte detectable in the specific methanolic extract.

Strictosidine was detected only in one Notopleura species (*N.siggersiana*). The metabolomics analysis revealed the presence of several strictosidine derivatives in *Rudgea* species. The species *R. skutchii* species contained strictosidinic acid (**20**), lyalosid (**21**), lyalosidic acid (**22**), deoxostrictosamide (**23**) and javaniside (**26**).

Metabolites 10-hydroxy strictosamide (**27**) and 10-hydroxy 3-epi strictosamide (**28**) were undistinguishable in mass analysis, they were detected in *R. laevis*, *R. cornifolia* and *R. raveniana*. Lyalosidic acid (**22**) was not only detected in *R. skutchii*, but also in *R. stipulacea*, deoxostrictosamide (**23**) occurred in *R. skutchii* and *R. cornifolia*. Strictosamide (**24**) was only found in *R. recurva*.

Table 25. Simplified results of metabolomic-profiling of methanolic leaf and stem material. Full information about the plant extracts are given in Table 3.

			compound								
genus	species	sample	**19**	**20**	**21**	**22**	**23**	**24**	**25**	**26**	**27/28**
Rudgea	*skutchii, leaf*	1351			•	•	•			•	
	skutchii,stem	1351			•		•			•	
	skutchii	211		•		•					
	skutchii	-		•							
	skutchii	1544		•							
	laevis	2026 (a)									•
	laevis	2024									•
	cornifolia	210210071					•				•
	cornifolia	1368									•
	raveniana	1413									•
	raveniana	1420									•
	recurva	1356						•			
	stipulacea	-				•					
Notopleura	*siggersiana*	1484	•								

strictosidine (**19**), strictosidinic acid (**20**), lyalosid (**21**), lyalosidic acid (**22**), deoxostrictosamide (**23**), strictosamide (**24**), vincosamide (**25**), javaniside (**26**), 10-hydroxy strictosamide (**27**), 10-hydroxy 3-epi strictosamide (**28**). Compound **27** and **28** could not be distinguished due to their identical molecular mass. *R. laevis* 2026 a and b are from the same sampling number but were stored in separate bags.

• analyte detectable in the specific methanolic leaf extract.

5 DISCUSSION

The natural compound isolation and characterization in *R. skutchii* and *R. raveniana* led to the identification of four known secoiridoid glycosides and two novel alstrostine derivatives. In the investigated *Rudgea* species, secologanin either forms secoiridoid glycosides or indole alkaloids in a ratio of 1:2 (indole : secologanin), additionally secoiridoid glycoside artefacts are built in the isolation progress. Strictosidine and or its derivatives could not be isolated, but strictosidine derivatives could be detected by metabolomics analysis in the leaf material of some *Rudgea* species.

5.1 Indole alkaloids (indole : secologanin 1:2)

The two alstrostine derivatives isoalstrostine B (**1**) and isoalstrostine C (**2**) were isolated and characterised for the first time in this work. Alstrostines were previously discovered in *Alstonia rostrata* (Cai et al., 2011), *Chassalia curviflora*, *Rudgea cornifolia* (Schinnerl et al., 2012) and *Palicourea luxurians* (Kornpointner et al., 2020).[9,13,20] The newly discovered alstrostines show the same core structure as the already known isoalstrostine, the sole difference is the additional caffeic acid attached to one glucose.

The novel isoalstrostine derivatives are an important addition to the alstrostine compound group. The presumed biosynthetic pathway is shown in Figure 4, it was postulated in 2011 by Cai et al. and adapted by Kornpointner et al., (2020).[20,13] The nitrogen heterocycle is formed by attack of the two secondary amines on the secologanins aldehyde units and the reaction of the C-3-aldehyde with the C-14' methylene group. In the biosynthesis the c1-path leads to isoalstrostines and the depicted c2-path results in alstrostines.[13] Concerning the caffeic acid, it is assumed that it is attached to the glucose after the formation of the isoalstrostine core structure. The attachment of phenolic compounds as caffeic acid are already known for strictosidine derivatives. Metabolites derived from strictosidine with a cinnamoyl acid attached to the glucose were isolated from *Palicourea padifolia* and *Palicourea adusta*.[44,48]

The more metabolites of the alstrostine group are discovered, the more the diversity and consequently the significance of this structural group is underlined. Compound **6** could not be isolated in sufficient amounts, making the structural elucidation difficult. In 4.10 the detailed analysis is described. The mass analysis lead

to the assumption of another isoalstrostines with two ester units at the iridoid moiety, the structural analysis could only confirm parts of the isoalstrostine structure. Based on the incomplete structure, compound **6** cannot be accounted for in the description of the isolated and described alstrostines, but it is once more an indicator of the variety of this structural group. The known alstrostines are shown in Figure 21.

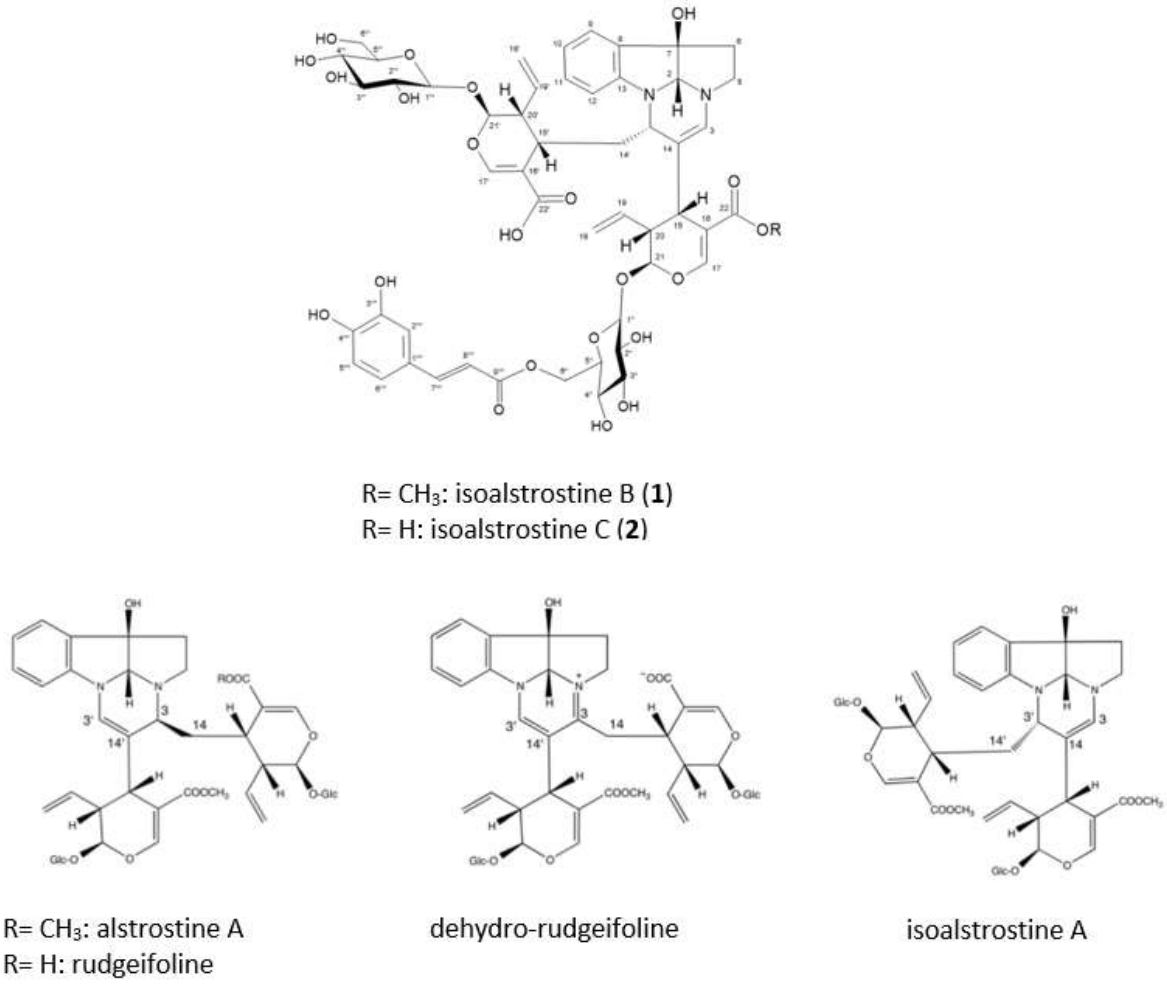

Figure 21. All six known alstrostines, alstrostines and isoalstrostines distinguish by the attachment of the second iridoid unit, which is a result of two possible biosynthetic routes. They are described in 1.2.3.

5.2 Secoiridoid glycosides

The variety of secoiridoid glycosides characterised in *R. skutchii* and *R. raveniana* indicates the presence of their precursor, secologanin. The fact that they are formed to this extend implies the accumulation of secologanin and individual metabolic pathways based on it. By intramolecular conversion of secologanin, sweroside (**9**) can be formed. The biosynthetic route is shown in Figure 22. The highly reactive aldehyde

function of secologanin forms the intermediate secologanic acid which then is reduced to sweroside by release of the hydroxy group.

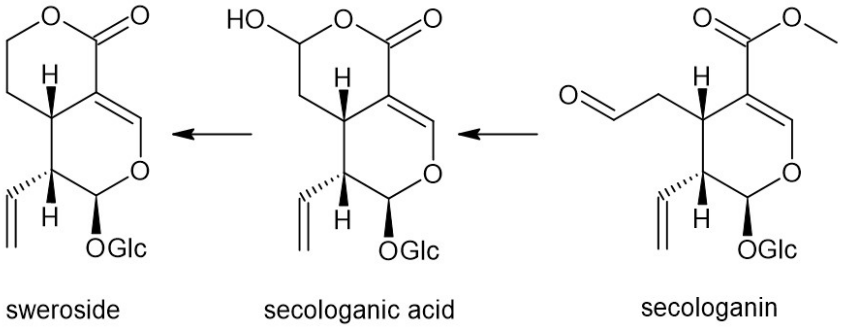

Figure 22. Biosynthetic route of sweroside from starting compound secologanin

The other secoiridoid glycosides **3**, **4**, **7**, **8** and **10** were not *in vivo* products of secologanin, they were assumed to be artefacts arisen during the isolation process. Methanol and *n*-butanol were both used in the liquid extraction process, thus leading to acetal formation with secologanin and resulting in the previously mentioned secologanin artefacts. The artefacts secologanin dibutylacetal, epi-vogeloside (**4** and **7**) and 7-*O*-butylsecologanic acid (**3** and **8**) are already known as typical reaction products emerging during the isolation process with methanol and *n*-butanol.[45] The high abundance of *in vivo* and *in vitro* artefacts of secologanin indicates the accumulation of secologanin.

In the work of Kornpointner et al. (2020), the different routes emerging from secologanin are discussed. The isolation process of *Palicourea luxurians* resulted in several secologanin derivatives formed by different routes with secologanin as starting point.[13] In this work, sweroside was the only i*n vivo* derivative of secologanin that could be isolated and characterised. The additional secoiridoid glycosides 7-*O*-butylsecologanic acid (**3**), epi-vogeloside (**4**) and secologanin dibutylacetal (**10**) were artefacts of the isolation process. Therefore, concerning the *Rudgea* species, little conclusions can be made about the variety of metabolic pathways originating from secologanin. But as previously discussed, the variety of *in vitro* artefacts speaks for a high abundance of secologanin in the plant tissue.

5.3 Metabolomic profiling focused on alkaloids

Alstrostine and its derivatives need tryptamine for their synthesis. The natural component which is derived from L-tryptophan is usually used by strictosidine synthase to form strictosidine. But the natural component isolation did not show any strictosidine derivatives in the investigated plant species. As already discussed in the work of Kornpointner et al., 2020, the activity of the STS-synthase is questioned in plant species synthesizing compounds of the alstrostine-type.[13] The fact that a variety of secoiridoid glycosides and alstrostines, which comprise two secologanin units, are produced by those plant species, underlines the presence of a considerable amount of secologanin which cannot be converted to strictosidine. The presence of the strictosidine-related 5α-carboxysrictosidine in *Palicourea luxurians* on the other hand claims the presence of a synthase catalysing the reaction of secologanin and L-tryptophan. Therefore, it is suggested to rename the strictosidine-synthase as Pictet-Spenglerase.[13]

It is of great interest whether alstrostine accumulating plant species are also able to biosynthesize strictosidine and therefore a variety of different derivatives originating from it. Using standard isolation and purification procedures with chromatographic methods could not reveal any strictosidine derivatives. MS metabolomics investigations were the method of choice used to discover even very small amounts of different metabolites in a diverse crude extract. An overlook of the results is shown in the supplement. Strictosidine was in fact not detected in any of the *Rudgea* species, but several of its derivatives in very little amount. 5α-carboxystrictosidine was also detectable in the leaf as well as the stem material of *Rudgea skutchii* (1351), which matches well as it was found in *Palicourea luxurians* next to alstrostines as well.[13] Its presence emphasizes the activity of an alternative synthase catalyzing the reaction of secologanin and L-tryptophan.

The fact that small amounts of strictosidine derivatives were found in the *Rudgea* species may indicate, that the strictosidine-synthase is in fact not totally inactive and produces strictosidine to very little extent. In relation to the amount of isolated isoalstrostine derivatives, the strictosidine derivatives may have very little meaning in the metabolism of the plant species. The biological purpose in metabolism may be taken over by alstrostines or other metabolites.

Considering the fact, that both isoalstrostines could not be detected in the crude extract (AB1351) they were isolated from, the analysis of this extract must be repeated in a higher concentration. Extensive investigations of crude extracts of several *Rudgea* and *Palicourea* species with metabolomics analysis must be carried out to get a profound answer to the question about the metabolism in alstrostine producing plants genus.

6 CONCLUSION

The intensive investigation of leaf and stem bark material of the three *Rudgea* species, *R. skutchii*, *R. laevis and R. raveniana* revealed two novel alstrostine derivatives, isoalstrostines B (**1**) and C (**2**). Furthermore, four secoiridoid glycosides (**3**–**4** and **9**–**10**) were identified in the plant tissue.

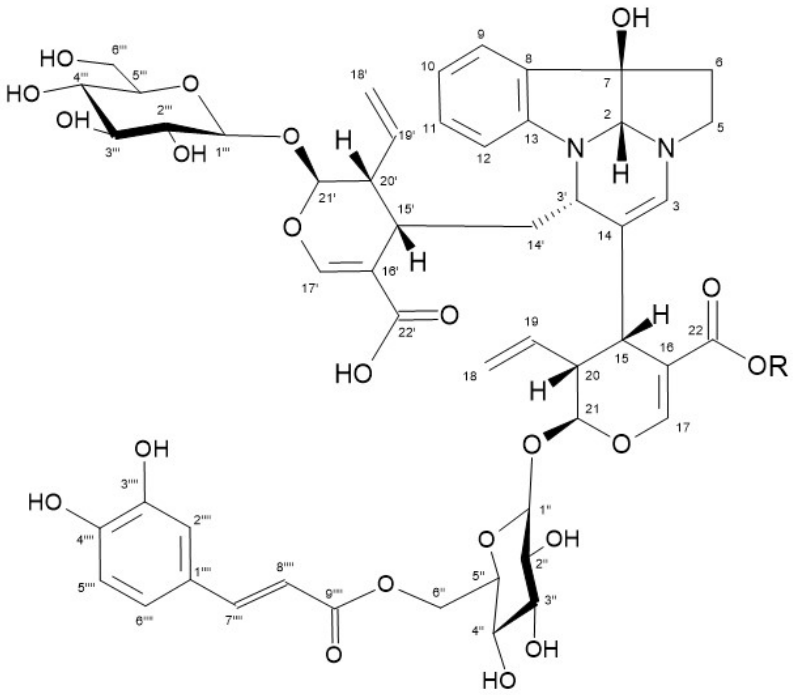

R = OCH_3: isoalstrostine B (**1**)
R = OH: isoalstrostine C (**2**)

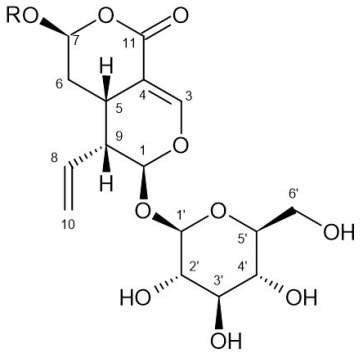

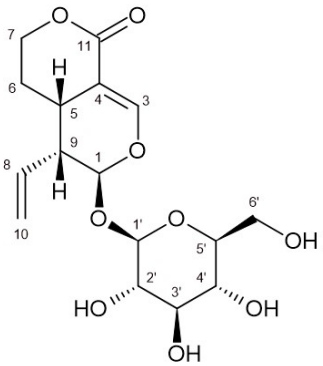

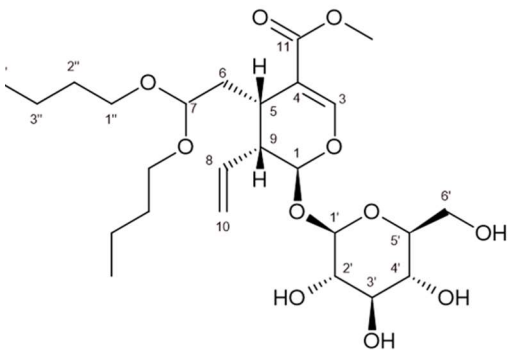

R = *butyl*: 7-*O*-butylsecologanic acid (**3**)
R = *methyl*: *epi*-vogeloside (**4**)

sweroside (**9**)

secologanin dibutylacetal (**10**)

Figure 23. Summary of all isolated and elucidated natural compounds.

The identified compounds are very similar to those yielded from *Palicourea luxurians*. Both plant species accumulate alstrostine derivatives and secoiridoid glycosides in their plant tissue and show none of the known strictosidine derivatives in higher amounts by the usual chromatographic isolation steps.[13]

Small amounts of strictosidine derivatives were found by metabolomic profiling in the *Rudgea* species. This may indicate that the strictosidine-synthase is in fact not totally inactive and produces strictosidine derivatives to very little extent. Another possibility is the presence of several different biosynthetic pathways leading to the strictosidine derivatives. Also, the Pictet-Spengler condensation can be catalyzed by different synthases with different substrate promiscuity and different outcome. In relation to the amount of isolated isoalstrostine derivatives, the strictosidine derivatives may have very little meaning in the metabolism of the plant species. The biological purpose in metabolism may be taken over by alstrostines or other metabolites.

In conclusion, the novel isoalstrostine are an important addition to the rather novel structural group of alstrostines. They underline the variety and therefore, importance of this novel biosynthetic pathway. The ratio of secologanin to tryptamine of 2:1 in alstrostines as well as the variety of secologanin derivatives indicate a high abundance of secologanin in the plant tissue. Secologanin that cannot be processed in the strictosidine pathway, or at least to very little extent.

7 MATERIALS AND CHEMICALS

7.1 Plant material

The plant material of *Rudgea skutchii* (1351), *R. raveniana* (1413) and *R. laevis* (D2024) was collected in the rainforest of south-eastern Costa Rica. In the area of La Gamba the association “Rainforest of the Austrians” founded a nature reserve under Michael Schnitzler to conserve threatened areas of the rainforest and even reforest cleared properties.[49]

7.2 Solvents and Chemicals

All chemicals and solvents were purchased from Merck, Sigma Aldrich or Carl Roth GmbH & Co.KG. There were no further purifications steps involved.

7.3 Chromatographic separation methods

TLC analyses were done on silica gel 60 F_{254} plates with a layer thickness of 0.2 mm on (Merck). They were developed with the organic phase of *n*-butanol/acetic acid/water 50:10:40 or with different mixtures of $CHCl_3$/MeOH. For preparative TLC, silica gel 60 F_{254} plates with a layer thickness of 0.25 mm were used. The layer of adsorbent is coated on glass. NPC was performed on silica gel 60 (Merck) with 40-60 µm particle size, eluted with mixtures of PE/EtOAc, $CHCl_3$/MeOH or EtOAc/MeOH. Sephadex LH-20 (GE Healthcare) with methanol as eluent was used for size exclusion chromatography. MPLC separations were done over a prepacked reversed phase silica gel column (LiChoprep Rp-18) using H_2O/MeOH mixtures. The pressure was regulated by a C-610/Pump module C-601 coupled with an UV-photometer.

7.4 Analytical instruments

HPLC analyses were performed on Agilent 1100 series using an UV-diode array detection and a Hypersil BDS-C18 column (250×4.6 mm, 5 µm particle size). The wavelength was set at 230 nm (reference WL 360 nm). The flow rate was set at 1 mL min^{-1}, the temperature was at 293 K and the injection volume was 10 µL. The eluent was an aqueous solution containing 10 mM ammonium acetate (A) and MeOH (B). The gradient was as following: From 20 to 90 % B in A within 15 min, within 0.1 min to 99 % B in A and 99 % B was kept for 9.6 min.

NMR analyses were performed on Bruker Avance III 600 at 600.13 MHz (^{1}H) or 150.61 MHz (^{13}C) with Topspin 3.5 software. Measurement temperature was 298 K ± 0.05 K. Compounds were dissolved in CH_3OD (~1.5 mg in 0.7 mL) and transferred in a precision NMR sample tube. The residual not fully deuterated solvent is also used as internal standard, MeOD for ^{1}H (δH 3.34) and CD_3OD for ^{13}C (δC 49.0) measurements. 1D spectra were recorded by acquisition of 32 k data points, zero filling to 64 k data points followed by Fourier transformation of spectra performed with a range of 7,200 Hz (^{1}H) and 32,000 Hz (^{13}C), respectively. The two-dimensional COSY, TOCSY, NOESY, ROESY, HSQC, and HMBC spectra were determined by 128 experiments with 2,048 data points each, they were Fourier-transformed to 2D-spectra with a range of 6,000 Hz and 32,000 Hz for ^{1}H and ^{13}C NMR, respectively.

Extinction E was determined by a Specord 205 photometer using a 10 mm quartz cuvette. The value of extinction was employed for calculating the molar extinction coefficient.

The optical rotation was measured at a sodium D line on a PerkinElmer Automatic Polarimeter 341. A 100 mm path length cell was used and the temperature was set at 20°C.

Mass spectra were recorded on a high-resolution time-of-flight (HR-TOF) mass spectrometer (maXis, Bruker Daltonics). Direct infusion electrospray ionization (ESI) was the ion source for positive and negative ionization mode. It is the result of capillary voltage of 4 kV to maintain a (capillary) current between 30-50 nA. The nitrogen temperature was kept at 180°C using a flow rate of 4.0 L min^{-1} and the N_2 nebulizer gas pressure at 0.3 bar.

For metabolomic profiling a Vanquish UHPLC coupled to ESI-Q Exactive HF-Q-Orbitrap was used. The LC eluent was a mixture of H_2O + 0.2 % formic acid (A) and MeOH + 0.2 % formic acid (B), the gradient was as following: In 0.3 min from 1 to 5 % B in A, followed by 40 % B in A at 5 min. within 0.1 min B was 80 %, was kept for 1.8 min and then in 0.1 min to 0 % B for 2 min. The injection volume was 10 µL and the flow rate 0.5 mL min^{-1}. Full MS was used with a scan range of 100 to 2000 *m/z* in both polarity modes. The resolution was set at 60 000, the capillary temperature was 250°C for positive and 320°C for negative mode.

8 REFERENCES

(1) Torres-Leite, F.; Bruniera, C. P.; Zappi, D. C.; Carrijo, T. T. A New Species of Rudgea (Palicoureeae, Rubiaceae) from Espírito Santo State, Brazil. *Phytotaxa* **2018**, *379* (2), 180–186. https://doi.org/10.11646/phytotaxa.379.2.6.

(2) Goevarts, R., Ruhsam, M., Andersson, L., Robbrecht, E., Bridson, D., Davis, A., Schanzer, I., Sonke, B. World checklist of Rubiaceae. Royal Botanic Gardens. Retrieved from http://www.kew.org/wcsp/ rubiaceae (retrieved 13.03.20).

(3) Robbrecht, E.; Manen, J. F. The Major Evolutionary Lineages of the Coffee Family (Rubiaceae, Angiosperms). Combined Analysis (NDNA and CpDNA) to Infer the Position of Coptosapelta and Luculia, and Supertree Construction Based on RbcL, Rps16, TrnL-TrnF and AtpB-RbcL Data. A New Class. *Syst. Geogr. Plants* **2006**, *76* (1), 85–146.

(4) Bremer, B.; Eriksson, T. Time Tree of Rubiaceae: Phylogeny and Dating the Family, Subfamilies, and Tribes. *Int. J. Plant Sci.* **2009**, *170* (6), 766–793. https://doi.org/10.1086/599077.

(5) Martins, D.; Nunez, C. V. Secondary Metabolites from Rubiaceae Species. *Molecules* **2015**, *20* (7), 13422–13495. https://doi.org/10.3390/molecules200713422.

(6) Gibbons, S.; Arunotayanun, W. Natural Product (Fungal and Herbal) Novel Psychoactive Substances. In *Novel Psychoactive Substances:Classification, Pharmacology and Toxicology*; Elsevier Inc., 2013; pp 345–362. https://doi.org/10.1016/B978-0-12-415816-0.00014-6.

(7) Razafimandimbison, S. G.; Taylor, C. M.; Wikström, N.; Pailler, T.; Khodabandeh, A.; Bremer, B. Phylogeny and Generic Limits in the Sister Tribes Psychotrieae and Palicoureeae (Rubiaceae): Evolution of Schizocarps in Psychotria and Origins of Bacterial Leaf Nodules of the Malagasy Species. *Am. J. Bot.* **2014**, *101* (7), 1102–1126. https://doi.org/10.3732/ajb.1400076.

(8) Torres-Leite, F.; Bruniera, C. P.; Zappi, D. C.; Carrijo, T. T. True Axillary Inflorescences in Rudgea (Palicoureeae, Rubiaceae), a Newly Reported Characteristic of Two New Brazilian Species, R. Quisquiliae and R. Axilliflora. *Phytotaxa* **2016**, *272* (3), 191–200. https://doi.org/10.11646/phytotaxa.272.3.3.

(9) Schinnerl, J.; Orlowska, E. A.; Lorbeer, E.; Berger, A.; Brecker, L. Alstrostines in

Rubiaceae: Alstrostine A from Chassalia Curviflora Var. Ophioxyloides and a Novel Derivative, Rudgeifoline from Rudgea Cornifolia. *Phytochem. Lett.* **2012**, *5* (3), 586–590. https://doi.org/10.1016/j.phytol.2012.05.019.

(10) Hänsel, R.; Sticher, O.; Steinegger, E. *Pharmakognosie-Phytopharmazie*, 6th ed.; Springer Verlag: New York, 1999.

(11) Panjikar, S.; Stoeckigt, J.; O'Connor, S. E.; Warzecha, H. The Impact of Structural Biology on Alkaloid Biosynthesis Research. *Nat. Prod. Rep.* **2012**, *29*, 1176–1200. https://doi.org/10.1039/c2np20057k.

(12) O'Connor, S. E.; Maresh, J. J. Chemistry and Biology of Monoterpene Indole Alkaloid Biosynthesis. *Nat. Prod. Rep.* **2006**, *23* (4), 532–547. https://doi.org/10.1039/b512615k.

(13) Kornpointner, C.; Berger, A.; Traxler, F.; Hadžiabdić, A.; Massar, M.; Matek, J.; Brecker, L.; Schinnerl, J. Alkaloid and Iridoid Glucosides from Palicourea Luxurians (Rubiaceae: Palicoureeae) Indicate Tryptamine- and Tryptophan-Iridoid Alkaloid Formation Apart the Strictosidine Pathway. *Phytochemistry* **2020**, *173* (February). https://doi.org/10.1016/j.phytochem.2020.112296.

(14) Tietze, L.-F. Secologanin, a Biogenetic Key Compound- Synthesis and Biogenesis of the Iridoid and Secoiridoid Glycosides. *Angew. Chem. Int. Ed. Engl.* **1983**, *22*, 828–841.

(15) Rohmer, M. The Discovery of a Mevalonate-Independent Pathway for Isoprenoid Biosynthesis in Bacteria, Algae and Higher Plants. *Nat. Prod. Rep.* **1999**, *16* (5), 565–574. https://doi.org/doi:10.1039/A709175C.

(16) Ida, Y.; Toriizuka, K.; Hirai, Y.; Ando, H.; Yamamoto, T.; Nakajima, Y.; Yamazaki, T.; Niiho, Y. Gastroprotective Effects of Bitter Principles Isolated from Gentian Root and Swertia Herb on Experimentally-Induced Gastric Lesions in Rats. *Nat. Med.* **2006**, *60*, 82–88. https://doi.org/10.1007/s11418-005-0014-2.

(17) Koudounas, K.; Thomopoulou, M.; Michaelidis, C.; Zevgiti, E.; Papakostas, G.; Tserou, P.; Daras, G.; Hatzopoulos, P. The C-Domain of Oleuropein ß -Glucosidase Assists in Protein Folding and Sequesters the Enzyme in Nucleus. *Plant Physiol.* **2017**, *174* (July), 1371–1383. https://doi.org/10.1104/pp.17.00512.

(18) Koudounas, K.; Banilas, G.; Michaelidis, C.; Demoliou, C.; Rigas, S.;

Hatzopoulos, P. A Defence-Related Olea Europaea β-Glucosidase Hydrolyses and Activates Oleuropein into a Potent Protein Cross-Linking Agent. *J. Exp. Bot.* **2015**, *66* (7), 2093–2106. https://doi.org/10.1093/jxb/erv002.

(19) https://roempp.thieme.de/lexicon/RD-19-01619 (retrieved on 02.09.20).

(20) Cai, X.; Bao, M.; Zhang, Y.; Zeng, C.; Liu, Y. A New Type of Monoterpenoid Indole Alkaloid Precursor from Alstonia Rostrata. *Org. Lett.* **2011**, *13* (14), 3568–3571.

(21) Stahl, E.; Schild, W. *Isolierung Und Charakterisierung von Naturstoffen*; Gustav Fischer Verlag: Stuttgart, New York, 1986.

(22) Breitmaier, E. *Alkaloide*, 3rd ed.; Vieweg + Teubner: Wiesbaden, 2008.

(23) Otterstätter, G. *Färbung von Lebensmitteln, Arzneimitteln, Kosmetika*, 3rd ed.; Behr's Verlag: Hamburg, 2007.

(24) Sangster, J. *Octanol-Water Partition Coefficients: Fundamentals and Physical Chemistry*; Wiley: West Sussex, 1997; Vol. 2.

(25) Gey, M. H. *Instrumentelle Analytik Und Bioanalytik Biosubstanzen, Trennmethoden, Strukturanalytik, Applikationen*, 3rd ed.; Springer Spektrum: Berlin Heidelberg, 2015. https://doi.org/10.1007/978-3-662-46255-3.

(26) Spangenberg, B. *Quantitative Dünnschicht- Chromatographie Eine Anleitung Für Praktiker*; Springer Spektrum: Berlin Heidelberg, 2014.

(27) Gray, A. I. *Natural Products Isolation*, 2nd ed.; Sarker, S. D., Latif, Z., Gray, A. I., Eds.; Humana Press: Totowa, 2006.

(28) Braun, T.; Ghersini, G. Extraction Chromatography. *J. Chromatogr. Libr.* **1975**, *2* (29), 584.

(29) Axén, R.; Porath, J. Chemical Coupling of Enzymes to Cross-Linked Dextran ('Sehadex'). *Nature* **1966**, *210*, 367–369.

(30) Handa, S. S.; Khanuja, S. P. S.; Longo, G.; Rakesh, D. D. *Extraction Technologies for Medicinal and Aromatic Plants*; International Centre for Science and High Technology: Trieste, 2008.

(31) Bruice, P. Y. *Organic Chemistry*, 8th ed.; Pearson Education, 2016.

(32) Otto, M. *Analytische Chemie*, 4th ed.; Wiley-VCH Verlag GmbH & CoKg, 2011.

(33) Hesse, M.; Meier, H.; Zeeh, B. *Spektroskopische Methoden in Der Organischen Chemie*, 7th ed.; Georg Thieme Verlag: Stuttgart, 2005.

(34) Claridge, T. D. W. *NMR Techniques in Organic Chemistry Third Edition*, 3rd ed.; Elsevier Ltd: Amsterdam, 2016.

(35) Friebolin, H. *Ein- Und Zweidimensionale NMR-Spektroskopie Eine Einführung*, 4th ed.; Wiley-VCH Verlag GmbH & CoKg, 2006.

(36) Editor, J. T. B.; Walker, J. M. *Metabonomics Methods and Protocols*; Editor, J. T. B., Ed.; Humana Press, 2015.

(37) Wishart, D. S.; Tzur, D.; Knox, C.; Eisner, R.; Guo, A. C.; Young, N.; Cheng, D.; Jewell, K.; Arndt, D.; Sawhney, S.; Fung, C.; Nikolai, L.; Lewis, M.; Coutouly, M.; Forsythe, I.; Tang, P.; Shrivastava, S.; Jeroncic, K.; Stothard, P.; Amegbey, G.; Block, D.; Hau, D. D.; Wagner, J.; Miniaci, J.; Clements, M.; Gebremedhin, M.; Guo, N.; Zhang, Y.; Duggan, G. E.; Macinnis, G. D.; Weljie, A. M.; Dowlatabadi, R.; Bamforth, F.; Clive, D.; Greiner, R.; Li, L.; Marrie, T.; Sykes, B. D.; Vogel, H. J.; Querengesser, L. HMDB : The Human Metabolome Database. *Nucleic Acids Res.* **2007**, *35*, 521–526. https://doi.org/10.1093/nar/gkl923.

(38) Schwaiger, M.; Schoeny, H.; El Abiead, Y.; Hermann, G.; Rampler, E.; Koellensperger, G. Merging Metabolomics and Lipidomics into One Analytical Run. *Analyst* **2019**, *144* (1), 220–229. https://doi.org/10.1039/c8an01219a.

(39) Dunn, W. B.; Broadhurst, D.; Begley, P.; Zelena, E.; Francis-mcintyre, S.; Anderson, N.; Brown, M.; Knowles, J. D.; Halsall, A.; Haselden, J. N.; Nicholls, A. W.; Wilson, I. D.; Kell, D. B.; Goodacre, R. Procedures for Large-Scale Metabolic Profiling of Serum and Plasma Using Gas Chromatography and Liquid Chromatography Coupled to Mass Spectrometry. *Nat. Protoc.* **2011**, *6*, 1060–1083. https://doi.org/https://doi.org/10.1038/nprot.2011.335.

(40) Raftery, D. *Mass Spectrometry in Metabolomics: Methods an Protocols*, 1198th ed.; Walker, J. M., Ed.; Springer Protocolls, 2014.

(41) Zhou, J.; Liu, H.; Liu, Y.; Liu, J.; Zhao, X.; Yin, Y. Development and Evaluation of a Parallel Reaction Monitoring Strategy for Large-Scale Targeted Metabolomics Quantification. *Anal. Chem.* **2016**, *88*, 4478–4486. https://doi.org/10.1021/acs.analchem.6b00355.

(42) Umfahrer, B. Isolation and Structure Elucidation of Secondary Metabolites of

Rudgea Raveniana and Their Effects on Generalist Insects, Bachelor Thesis University of Vienna, 2020.

(43) https://www.nmrdb.org/ (retrieved 10.05.2020).

(44) Berger, A.; Kostyan, M. K.; Klose, S. I.; Gastegger, M.; Lorbeer, E.; Brecker, L.; Schinnerl, J. Loganin and Secologanin Derived Tryptamine-Iridoid Alkaloids from Palicourea Crocea and Palicourea Padifolia (Rubiaceae). *Phytochemistry* **2015**, *116* (1), 162–169. https://doi.org/10.1016/j.phytochem.2015.05.013.

(45) Tomassini, L.; Cometa, M. F.; Serafini, M.; Nicoletti, M. Isolation of Secoiridoid Artifacts from Lonicera Japonica. *J. Nat. Prod.* **1995**, *58* (11), 1756–1758. https://doi.org/10.1021/np50125a020.

(46) Recio-Iglesias, M.-C.; Marston, A.; Hosteyitmann, K. Xanthones and Secoiridoid Glucosides of Halenia Campanulata. *Phytochemistry* **1992**, *31* (4), 1387–1389.

(47) Berger, A.; Tanuhadi, E.; Brecker, L.; Schinnerl, J.; Valant-Vetschera, K. Chemodiversity of Tryptamine-Derived Alkaloids in Six Costa Rican Palicourea Species (Rubiaceae–Palicoureeae). *Phytochemistry* **2017**, *143*, 124–131. https://doi.org/10.1016/j.phytochem.2017.07.016.

(48) Valverde, J.; Tamayo, G.; Hesse, M. SS-Carboline Monoterpenoid Glucosides from Palicourea Adusta. *Phytochemistry* **1999**, *52*, 1485–1489.

(49) https://www.regenwald.at (retrieved on 20.08.20).

9 LIST OF FIGURES

10 LIST OF TABLES

11 SUPPLEMENT

Metabolomics results concluded in a single table. The results as well as the compound names for 1-28 are also listed in 4.11.

genus	*species*	sample	organ	**1**	**2**	**11**	**13**	**14/15**	**16**	**17**	**18**	**19**	**20**	**21**	**22**	**23**	**24**	**25**	**26**	**27/28**
Rudgea	*jasminoides*	4712	leaf	•																
	parquioides	339	leaf					•												
	stipulacea	-	leaf												•					
	skutchii	1544	leaf										•							
	skutchii	-	leaf										•							
	skutchii	211	leaf										•		•					
	skutchii	1351	leaf				•							•	•	•			•	
	skutchii	1351	stem				•							•		•			•	
	cornifolia	210210071	stem													•				•
	cornifolia	1368	stem																	•
	raveniana	1413	leaf																	•
	raveniana	1420	leaf																	•
	laevis	2026 (a)	leaf		•	•														•
	laevis	2024	leaf			•														•
	laevis	2026 (b)	leaf			•														
	reducticalyx	1473	leaf			•														
	ciliata	28020	leaf			•														
	recurva	1356	leaf			•											•			
Notopleura	*anmothyrsa*	7021001	leaf			•														
	siggersiana	1484	leaf			•						•								

Mass spectra of the novel compound isoalstrostine B in positive (li) and negative (re) mode.

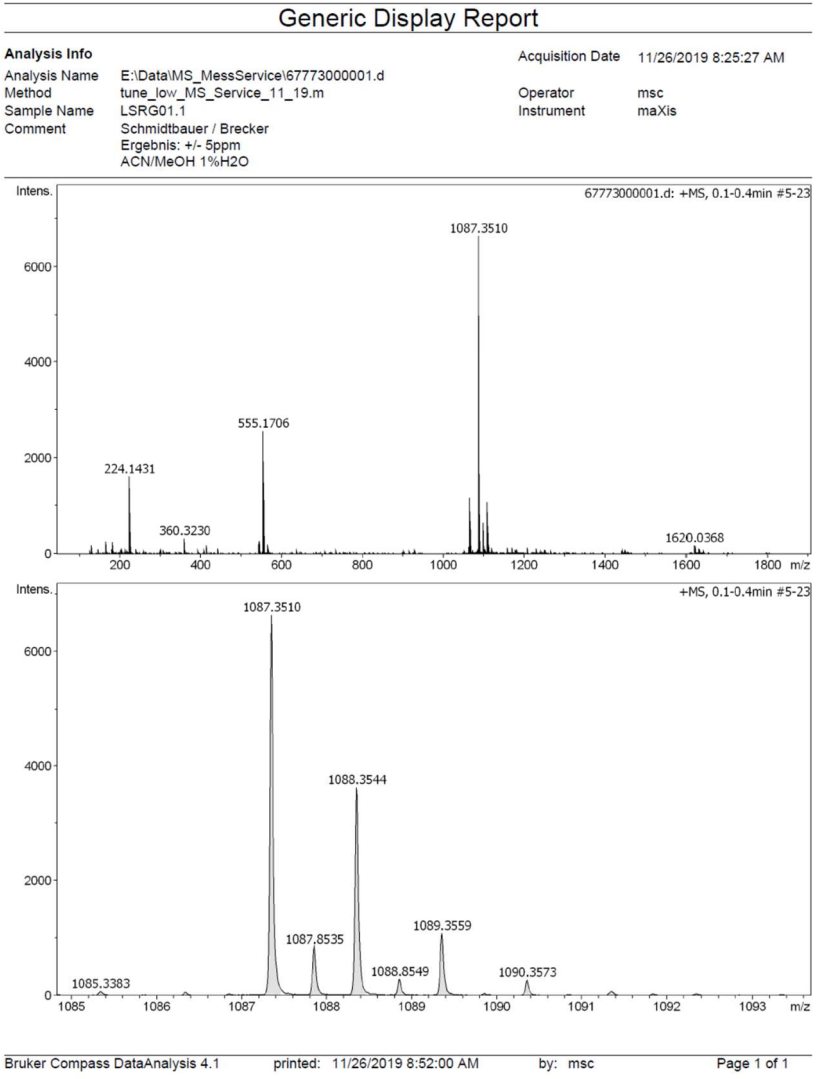

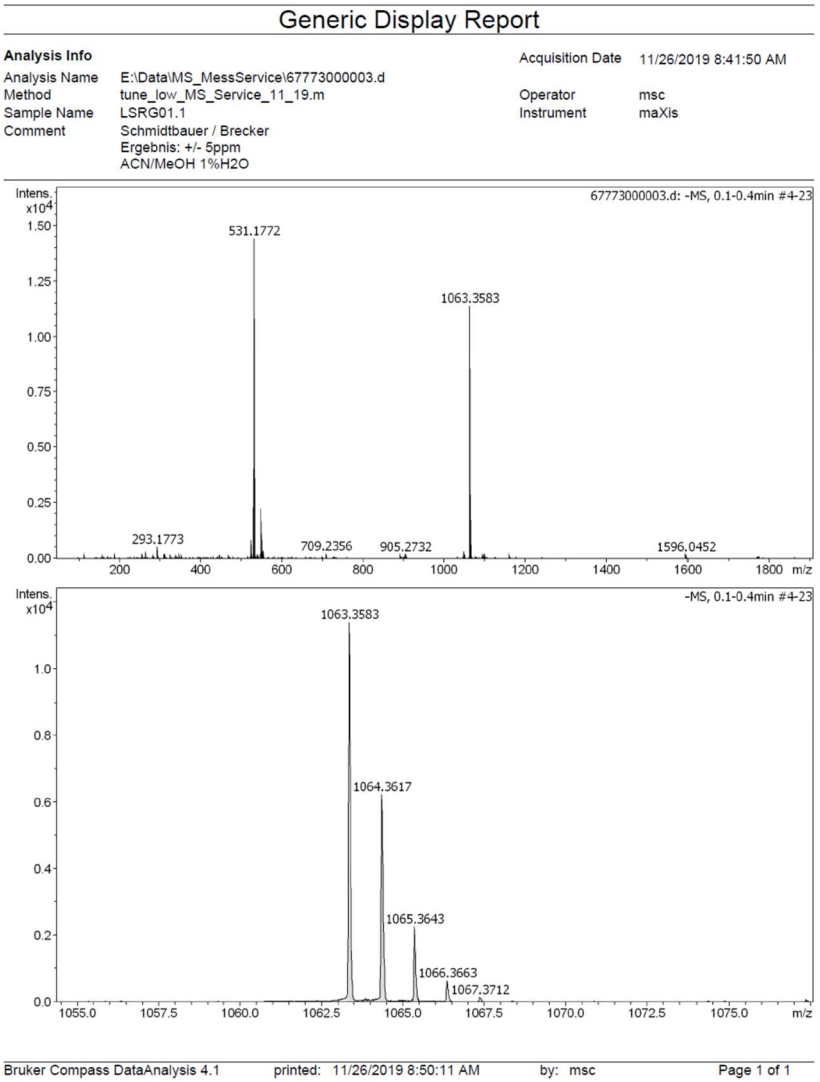

Mass spectra of the novel compound isoalstrostine C in positive (li) and negative (re) mode.